Journal of Inflammation Research

Dovepress
Taylor & Francis Group

Open Access Full Text Article

ORIGINAL RESEARCH

To Explore the Mechanism of Cuproptosis in Psoriasis Based on Bioinformatics and in vivo Experiments

Yingying Ma[1,*], Ying Sun[2], Jintong Yao[3], Jian Zhang[4,*], Hailiang Wang[2], Suqing Yang[5]

[1]Department of First Clinical Medicine, Heilongjiang University of Chinese Medicine, Harbin, Heilongjiang, People's Republic of China; [2]Department of Dermatology, Affiliated Hospital of Changchun University of Traditional Chinese Medicine, Jilin, Changchun, People's Republic of China; [3]Department of Internal Medicine, Northeast Electric Power University, Jilin, Jilin, People's Republic of China; [4]Department of Basic Medicine, Heilongjiang University of Chinese Medicine, Harbin, Heilongjiang, People's Republic of China; [5]Department of Dermatology, The First Affiliated Hospital of Heilongjiang University of Traditional Chinese Medicine, Harbin, People's Republic of China

*These authors contributed equally to this work

Correspondence: Suqing Yang, Department of Dermatology, The First Affiliated Hospital of Heilongjiang University of Traditional Chinese Medicine, No. 24, Heping Road, Harbin, Heilongjiang, 10054, People's Republic of China, Email ysq_6410@163.com

Purpose: To explore the mechanism of cuprotosis in psoriasis, screen cuprotosis related genes (PDCRGs) in psoriasis, and provide new targets for precise diagnosis and treatment of psoriasis.

Material and Methods: Integrate bioinformatics analysis and experimental validation. Firstly, based on the GEO database (GSE161683, GSE166388, GSE277173), differentially expressed genes (DEGs) and weighted gene co-expression network analysis (WGCNA) in psoriasis were screened; Identification of differential cuprotosis related genes (PDCRGs) in psoriasis using a self built cuprotosis gene database (1098 CRGs); Screen key PDCRGs through PPI network, machine learning, and ROC analysis. Subsequently, a mouse model of psoriasis induced by imiquimod (IMQ) was constructed, and gene expression, copper ion levels, inflammatory factors, and oxidative stress factors were validated using qPCR, Western blot, immunohistochemistry, fluorescence, and ELISA.

Results: Thirty-four PDCRGs were identified, among which STAT1, DLD, GBP1, CXCL10, PDHB, and LIAS are Hub genes. Machine learning and ROC analysis further identified APOL6, CD274, and LIAS as key diagnostic biomarkers. PDCRGs are significantly enriched in the TCA cycle, copper ion transport, and glucose metabolism pathways. The levels of FDX1 and serum copper ions were increased in the skin lesions of psoriasis mice, accompanied by upregulation of TCA cycle key proteins and PDCRGs expression; Copper overload triggers oxidative stress and inflammation cascade.

Conclusion: APOL6, CD274, and LIAS were screened as cuprotosis markers in psoriasis. Overexpression of these PDCRGs in psoriasis model mice can promote copper ion accumulation and interfere with the TCA cycle, increase oxidative stress and inflammation levels, and ultimately lead to the occurrence of psoriasis. Therefore, targeted intervention of cuprotosis is of great significance for the clinical treatment of psoriasis.

Keywords: psoriasis, cuprotosis, immune inflammation, oxidative stress, bioinformatics

Introduction

Psoriasis is a systemic immune-mediated disease characterized by chronic inflammatory skin lesions, clinically manifested as well-defined erythematous and scaly plaques, accompanied by abnormal proliferation and differentiation disorders of keratinocytes.[1–3] About 2–3% of the global population is affected by it, and there are significant regional differences in the incidence rate. The Caucasian population can reach 11%, while the Asian and African populations are relatively lower. This disease has strong genetic susceptibility, and its pathogenesis involves multiple interactions between innate and adaptive immune systems. Dendritic cells recognize their own nucleic acid antimicrobial peptide complexes (such as LL37-DNA) through TLR7/9 activation, thereby promoting the IL-23/IL-17 axis dominated inflammatory cascade.[4,5] The key cytokines

Received: 2 October 2025
Accepted: 6 November 2025
Published: 13 December 2025

TNF-α, IL-17, and IL-23 drive excessive proliferation of keratinocytes, forming a vicious inflammatory cycle.[6] Although targeted biologics such as anti-IL-17/IL-23 monoclonal antibodies have been applied in clinical practice, the infection risk and efficacy limitations caused by their immunosuppressive effects still need to be urgently addressed.[7]

Cuproptosis is a newly discovered programmed cell death mechanism in 2022, triggered by abnormal accumulation of copper ions within cells. Its mechanism is different from classical pathways such as apoptosis and ferroptosis. Excessive Cu^2+ enters mitochondria through ion carriers and is reduced to Cu+ by ferredoxin-1 (FDX1). The latter binds to thiocyanate proteins (such as DLAT) in the tricarboxylic acid cycle, causing toxic aggregation and leading to mitochondrial respiratory chain collapse and Fe-S cluster protein instability.[8–11] The imbalance of copper homeostasis is closely related to various diseases such as cancer, heart disease, Alzheimer's disease, etc. The effectiveness of copper ion carrier Elesclomol in tumor treatment suggests that cuprotosis may become a new target for disease intervention.[12] It is worth noting that this pathway of death is highly dependent on mitochondrial respiratory function and is fundamentally associated with energy metabolism disorders and oxidative stress damage.

In the past few years, various programmed cell deaths (PCDS), including apoptosis, pyroptosis and ferroptosis, have been found to be closely related to the pathological process of psoriasis. In psoriasis, apoptosis is inhibited, the expression of Caspase-9 is decreased and the anti-apoptotic protein Bcl-2 is upregulated, resulting in abnormal proliferation of keratinocytes. Ferroptosis is activated by iron metabolism disorders and lipid peroxidation, promoting the accumulation of reactive oxygen species and inflammatory responses. Pyroptosis is mediated by gasdermin protein and Caspase-1, triggering intense inflammation in keratinocytes and macrophages and exacerbating skin damage. However, although existing studies have revealed the mechanisms by which these PCDS promote the progression of psoriasis, these PCDS have obvious drawbacks, including the unclear pro-anti-balance mechanism of death, the need for in-depth exploration of biological effects, and the unstable efficacy of targeted therapy. As a newly discovered form of copper-dependent programmed death, cuprotosis may be related to the pathology of psoriasis. It is particularly necessary to explore the mechanism of cuprotosis, which may provide key evidence for revealing new pathogenic pathways and developing innovative therapies. The potential link between psoriasis and cuproptosis stems from the intersection of three mechanisms. Firstly, there is significant mitochondrial dysfunction in the psoriasis lesion area, and the oxidative stress microenvironment can promote copper ion accumulation.[13,14] Secondly, the key regulatory factor of cuproptosis, FDX1, is involved in inflammatory signaling, and its abnormalities may amplify the effects of the IL-17/IL-23 pathway.[15] Finally, copper ions affect keratinocyte proliferation and immune cell activation by regulating transcription factors such as NF-κB.[16,17] Research has shown that upregulation of the expression of the core transcription factor RORγt in Th17 cell differentiation is positively correlated with the severity of psoriasis, while copper homeostasis imbalance can directly affect the ligand binding domain activity of RORγt.[18] More noteworthy is that copper induced mitochondrial protein toxicity stress may synergize with inflammatory factors such as TNF-α to exacerbate epidermal barrier disruption and immune cell infiltration.[19]

The systematic identification of cuproptosis related genes in psoriasis can reveal how copper homeostasis imbalance participates in the maintenance of chronic inflammation in psoriasis through the mitochondrial immune axis, providing new ideas for cross disciplinary research on "metabolism immunity". At the therapeutic level, interventions targeting cuprotosis core molecules such as FDX1 and DLAT (such as copper chelators or small molecule inhibitors) may break through the efficacy bottleneck of existing biologics. At the clinical translation level, the construction of disease typing and prognosis models based on cuproptosis gene profiles will provide molecular markers for precise treatment of psoriasis. Therefore, this study aims to elucidate the pathological contribution of cuproptosis in psoriasis by integrating multi omics analysis and experimental verification, laying a theoretical foundation for the development of novel therapeutic strategies targeting cuproptosis pathways (Figure 1).

Materials and Methods

Screening of Cuproptosis Related Genes

Data Collection

The samples from the merged GSE161683 and GSE166388 datasets have been used for comprehensive analysis in machine learning. Using "psoriasis" as a keyword in the comprehensive gene expression database (https://www.ncbi.nlm.nih.gov/

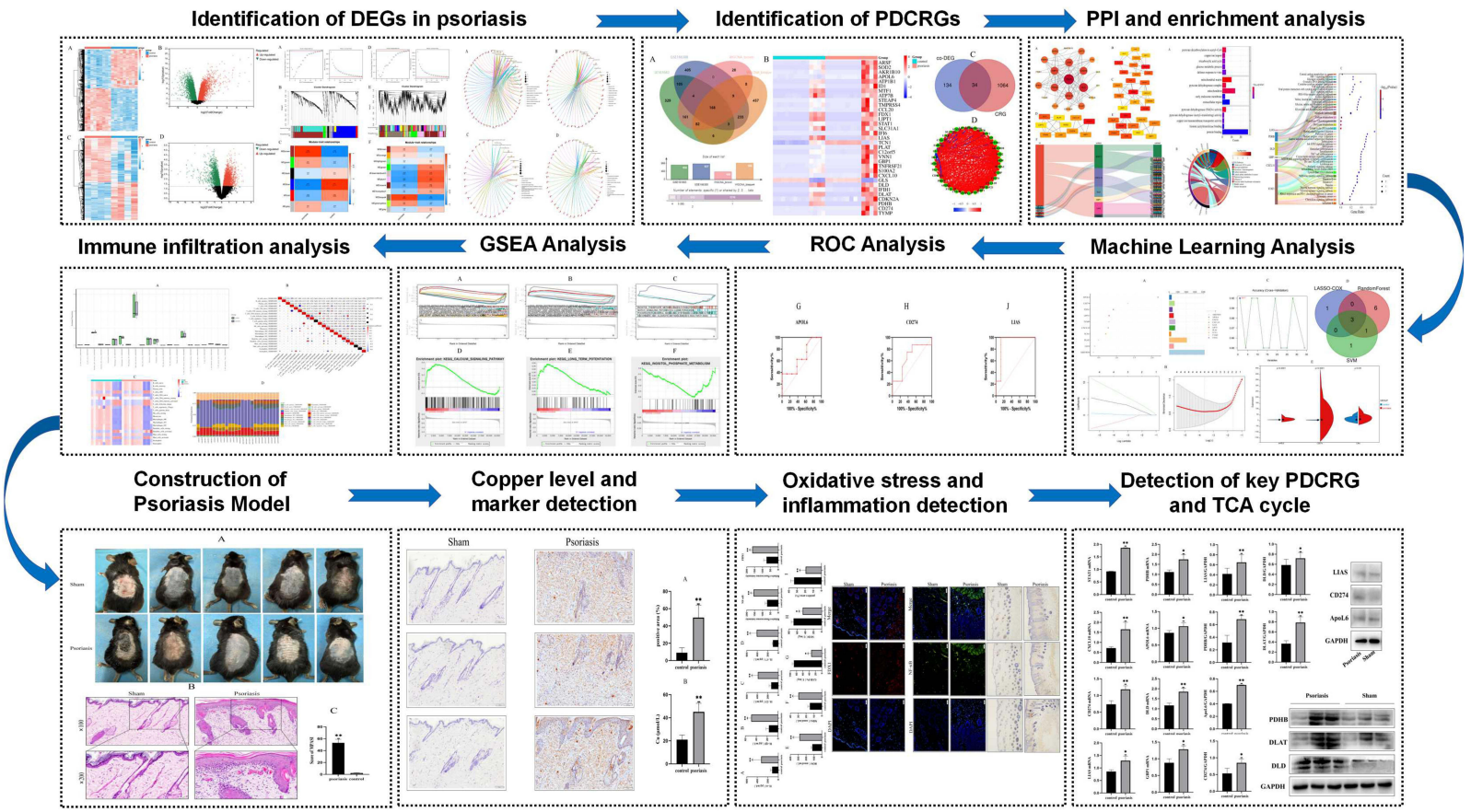

Figure 1 The workflow of this study.

home/genomes/). Finally, three datasets were selected, including GSE277173 (from GPL11532 platform, 8 psoriasis patient samples and 8 healthy control samples), GSE161683 (from GPL6244 platform, 9 psoriasis patient samples and 9 healthy control samples), and GSE166388 (from GPL570 platform, 4 psoriasis patient samples and 4 healthy control samples). Among them, GSE161683 and GSE166388 are used as training datasets, while GSE277173 is used as an external validation dataset. We use R software for quality control of the dataset, specifically by converting probe names to gene names, removing duplicate genes and null expressions, and performing batch normalization on each dataset. The collection of cuproptosis related genes (CRGs) mainly comes from self built databases, specifically relying on previously published literature reports and the Genecard database (https://www.genecards.org/) and through searching the GSEA database (www.gsea-msigdb.org).[20–23] In the Genecard and GSEA databases, we used cuproptosis as the search keyword. "Protein Coding" and "Relevance Score > 0" were used as the conditions for collecting CRGs in Genecard, and "FDR q-val < 0.25" was used as the condition for collecting CRGs in GSEA. Eventually, a total of 1098 CRGs were obtained.

Differential Expression Gene (DEG) Analysis

Using the limma package of R software (version 4.4.1) to screen the DEGs of GSE161683 and GSE166388. Construct a design matrix based on sample grouping, fit the expression data using lmFit(), and perform empirical Bayesian correction using eBayes; The screening of significantly different genes applies a dual threshold, with an adjusted p-value <0.05 and an absolute $\log_2$ fold change (|logFC|) > 1; The visualization of results includes using "ggplot2" to draw volcano maps and "heatmap" to draw heatmaps.[24,25]

Weighted Gene Co-Expression Network (WGCNA) Analysis

This study is based on the GSE161683 and GSE166388 datasets, and uses the R package WGCNA (v1.72) to construct weighted gene co expression networks. Firstly, genes with expression variance values above the 75th percentile are screened for subsequent analysis. The optimal soft threshold β is determined through scale-free topological fitting (fitting index threshold > 0.8), and a Pearson correlation weighted adjacency matrix is constructed and transformed into a topological overlap matrix (TOM). Using the dynamic tree cutting algorithm (minimum module size = 20, cutting sensitivity = 2) to identify co expressed modules and merge redundant modules with feature vector similarity >0.75. Furthermore, calculate the correlation between module feature genes (ME) and target traits, and screen for significantly correlated modules (Pearson correlation coefficient | r | > 0.3 and p < 0.05). Finally, hub genes are extracted from the target module, which must meet the dual screening criteria of intra module connectivity (kME > 0.8) and gene significance (| GS | > 0.2).[26]

Differential Cuproptosis Related Gene Screening in Psoriasis (PDCRGs)

Upload the obtained DEGs, the most significant related module genes, and the CRGs from the self built cuproptosis related gene data to the bioinformatics and evolutionary genomics platform (https://bioinformatics.psb.ugent.be/) Filter out DCRGs and draw Venn plots.

Protein-Protein Interactions (PPI) and Enrichment Analysis

Import the obtained PDCRGs into the STRING database (https://cn.string-db.org) set the biological species option to "Homo sapien" and the minimum interaction threshold to "Highest confidence>0.9", and download the tsv format file. The tsv file was imported into Cytoscape 3.9.1 software, free nodes were removed, Hub PDCRGs were screened using the CytoHubba plugin, and a visual PPI network was constructed. Subsequently, PDCRGs were uploaded to the DAVID database (https://david.ncifcrf.gov/tools.jsp) perform gene ontology (GO) and Kyoto Encyclopedia of Genes and Genomes (KEGG) analysis, with p-value <0.05 as the condition, to screen for biological processes (BP), molecular functions (MF), cell composition (CC), and pathway enrichment results, and draw enrichment analysis maps in R language.

Machine Learning Analysis

Using integrated machine learning strategy to screen key biomarkers for pre screened PDCRG. Firstly, through random forest (RF) analysis, the importance of gene Gini coefficient was iteratively calculated using 500 decision trees, retaining the top 10% of genes with importance scores. Using LASSO-COX regression, optimize the lambda value under 10 fold

cross validation and lambda value >0 is selected as the key genes screening condition. Finally, support vector machine (SVM) is used to recursively eliminate features using radial basis kernel function for gene sorting. We select the top 10 genes that can be retained when the model performance reaches its peak for cross-validation. By integrating the results of three algorithms, the top 10 hub genes that repeatedly appear and rank high in the three methods were extracted as core candidate biomarkers for cuproptosis regulation.[27]

Receiver Operating Characteristic (ROC) Analysis

For the PDCRG screened in the early stage, the pROC package (v1.18.0) was used for ROC analysis to verify its diagnostic efficacy. Firstly, the optimal expression cutoff values for each gene are determined by the maximum Youden index; Further calculate the area under the curve (AUC) and its 95% confidence interval, with the evaluation criteria being AUC > 0.6 and p-value < 0.05; Finally, the collaborative diagnostic performance of the hub gene set was validated through multi gene joint ROC analysis.

Gene Set Enrichment (GSEA) Analysis

Convert the probe names in the PDCRG series expression matrix into gene names, remove abnormal and non gene name data, and then upload them to the Gene set enrichment analysis (GSEA) software (v3.0) for ssGSEA analysis of key PDCRGs. Based on gene expression profiles and phenotype grouping, set the minimum gene set to 5 and the maximum gene set to 500, 1000 resamples, p-value < 0.05, FDR of <0.25.

Immune Infiltration Analysis

Using the CIBERSORT to perform immune microenvironment analysis on pre screened PDCRG. Based on the PDCRG standard expression profile, the proportion of various types of immune cells in the sample is calculated by deconvolution using the LM22 feature matrix. Data preprocessing includes quantile normalization of expression levels and batch effect correction; Furthermore, for each differentially expressed cuprotosis gene, calculate the rank correlation coefficient between its expression level and immune cell abundance, and identify significantly correlated immune cell subgroups; Finally, the key gene immune cell interaction network was displayed through heatmap visualization.[28]

Verification of Cuproptosis Related Genes

Animal Modeling and Grouping

Ten C57BL/6 mice aged 6 weeks were purchased from Liaoning Changsheng Biotechnology Co., Ltd. (SCXK (Liao) 2020–0001), with half male and half female, weighing 20 ± 5 g, and were placed in an SPF animal room for adaptive feeding for one week. The determination of the sample size is ultimately based on the detection method and indicators. According to the random number table method, mice were divided into Sham group (5 mice) and psoriasis group (5 mice). Then, the back hair of each group of mice was removed, exposing 6 cm^2 of surface skin. The sham group rats were locally applied vaseline lubricant daily, while the psoriasis group mice were applied 62.5 mg of 5% Imiquimod (IMQ, Tianfang Pharmaceutical Co., Ltd., Lot: 241203003) cream once a day for 7 consecutive days.[29] This animal experiment has been approved by the animal experiment ethics committee of Heilongjiang University of Traditional Chinese Medicine (SYXK-20250606), and all procedures involving the use of experimental animals comply with ethical requirements. We declare that in this study we adhered to the ARRIVE guidelines. After the completion of modeling, excessive pentobarbital sodium anesthesia was used to collect blood from the abdominal aorta of mice. Subsequently, the mice were euthanized by decapitation and the skin lesion tissue on the back was quickly peeled off. One part was fixed in 4% paraformaldehyde neutral buffer for 24 h and used for histopathological testing, while the other part was stored in −80 for testing of other indicators.

Mice Psoriasis Area and Severity Index (MPASI)

MPASI is a standardized quantitative tool used to assess the severity and extent of psoriasis lesions in mice. Animals are divided into five regions: head, upper limbs, trunk, lower limbs, and tail. The scores for each region are calculated using a formula (skin lesion area score × [erythema score+infiltration score+scale score] × region weight coefficient), and the

total score (0–72 points) is obtained by adding the scores of the five regions. The higher the score, the more severe the overall severity of psoriasis.[30]

HE Staining

Fixed skin tissue samples were embedded in paraffin. After preparing 4 μm continuous sections and spreading them in a 60°C oven, they were sequentially subjected to xylene dewaxing (twice, each for 10 min), gradient ethanol rehydration (100%, 95%, 90%, 80%, 70%, each for 5 min), hematoxylin staining for 5 min, 1% hydrochloric acid ethanol differentiation for 3 seconds, 0.5% ammonia water blue return for 30 seconds, 0.5% eosin staining for 1 min, followed by gradient ethanol dehydration and xylene transparency. Finally, they were sealed with neutral gum and observed for the pathological characteristics of epidermal psoriasis under an optical microscope. And the pathological morphology of the tissue was evaluated using the blinding method.

Immunohistochemical Staining

Based on the operation in section 2.2.1, paraffin sections of skin tissue were dewaxed and treated with gradient ethanol, and then repaired using sodium citrate; After incubating at room temperature with 3% H2O2 for 15 min and blocking non-specific sites with 5% BSA for 30 minutes, SLC31A1 and ATP7B primary antibodies (1:800, Abcam (Shanghai) Trading Co., Ltd, Cat: ab133385, ab240880) were added dropwise and incubated overnight in a 4°C wet box; Subsequently, the secondary antibody was incubated at room temperature for 1h, followed by the addition of DAB staining solution and rinsing with distilled water. Hematoxylin staining was performed for 1 min, followed by differentiation with 0.1% hydrochloric acid ethanol for 5 s. After dehydration and transparency, neutral gum was used for fixation, and the positive area was calculated using Image J.

Immunofluorescence Staining

Following the method described in 2.2.1, skin tissue paraffin sections were subjected to xylene dewaxing and gradient ethanol rehydration, followed by microwave repair using EDTA antigen repair buffer for 10 min. After 15 min of permeabilization treatment with 0.1% Triton X-100 and 30 min of blocking with 5% donkey serum, FDX1 (1:500, Wuhan Sanying Biotechnology Co., Ltd, Cat: 12592-1-AP) and NF-κB primary antibody (1:500, Shanghai Beyotime Biotechnology Co., Ltd, Cat: AB2020) were added dropwise and incubated overnight in a 4°C wet box in the dark. The next day, the fluorescent labeled secondary antibody (1:500) was incubated at room temperature in the dark for 1 hour, and DAPI stained the nuclei for 5 minutes; Finally, the film was sealed with anti fluorescence quenching sealing agent, and images were collected under a fluorescence microscope (Zeiss LSM 900). The fluorescence intensity was analyzed using Image J.

ELISA

Centrifuge the blood sample obtained in 2.2.1 at 15000r/min for 10 min, collect the supernatant, follow the instructions of the kit to detect the absorbance of Cu, IL-1 β, IL-6, IL17, IL23, ROS, SOD, GSH-Px (Shanghai Enzyme-linked Biotechnology Co., Ltd, Cat:ml103491, mI098430, ml263818, ml220179, ml161104, ml106717, ml037757), and MDA (Shanghai Beyotime Biotechnology Co., Ltd, Cat:S0131S) in the serum of each group of mice. Calculate the expression levels of inflammation, oxidative stress, and copper in the serum.

qPCR

About 20 mg of mouse skin tissue was rapidly ground into powder in a liquid nitrogen pre cooled mortar, and TRIzol was added to extract total RNA. Take 1 μg of total RNA and perform reverse transcription using SuperScrip IV kit (Thermo Fisher Scientific Inc., Cat: 12594100) at 37°C for 15 min; 85°C, 5 s), synthesized cDNA; specific primers were designed using Primer BLAST for the target genes *STAT1, DLD, GBP1, CXCL10, PDHB, APOL6, CD274 and LIAS*. The primers were amplified using SYBR Green Master Mix (Thermo Fisher Scientific Inc., Cat: A46110) in the CFX96 Touch system (Bio Rad), pre denatured at 95°C for 3 min, followed by 40 cycles (95°C, 10 s; 60°C, 30 s), and finally verified for amplification specificity through melting curve analysis. Calculate the relative gene expression level using the $2^{-\Delta\Delta Ct}$ method. The primer sequences of all the target genes are shown in Table 1.

Table 1 Primer Sequence

Gene	Sequence	SIZE (bp)
STAT1	F:CATCCTGACCAACCTGTCCA R:TGGTGTCGGTAGGTCAAGTG	150
DLD	F:GCTGGAGGAGTTCAAGGTGA R:TGCTGTCACAGGCATTCATC	142
GBP1	F:TGGCTTTGGAGAGGAAGATG R:CTTCCGGTTCTGGAAGATCC	118
CXCL10	F: CCACGTGTTGAGATCATTGC R:GCTTCCCTATGGCCCTCATT	185
PDHB	F:GGCTGGTGATGGTGAAGAGT R:GGTGATGCCAGAGGTAGGAA	127
APOL6	F:CAGCCTCAGCAAGACCACTA R:GCCTGGGTAGGTGTTGTTGT	168
CD274	F:TGCAGACTTCAGCAAACCAC R:TGGCTCCCAGAATTACCAAG	105
LIAS	F:TCCGAGATGGACCTGACTGT R:ATCGGGAGAGGTTGTCACCT	192

Western Blot

Weigh 100 mg of mouse skin tissue and cut it into pieces. Add RIPA lysis buffer (Shanghai Beyotime Biotechnology Co., Ltd., Cat: P0013C) for homogenization and lysis. The protein concentration was measured using the BCA method, and after adding the sample buffer, it was mixed and heated for denaturation. SDS gel electrophoresis at constant pressure, wet rotation method was used to transfer the membrane onto the polyvinylidene fluoride membrane. About 5% concentration skim milk powder solution was sealed for 2.5 hours, and TBST was washed twice for 5 minutes each time. Add APOL6, CD274, LIAS, DLD, PDHB (Abcam (Shanghai) Trading Co., Ltd, Cat:ab92273, ab205921, ab96302, ab182146, ab155996) and DLAT (Wuhan Sanying Biotechnology Co., Ltd, Cat:13426-1-AP) primary antibodies separately and incubate overnight at 4°C, the antibody dilution ratio is 1:1000. Then incubate PVDF membrane with HRP labeled secondary antibody at room temperature for 1 h, and finally add ECL developer for development, and use gel imager to collect pictures. Using β-actin as an internal reference control, Image J software was used to calculate the ratio of the grayscale values of the target protein to the internal reference protein.

Results

Results of DEG Analysis for Psoriasis

In order to clarify the changes in differentially expressed genes in psoriasis patients, we performed differential analysis on GSE161683 and GSE166388 using p-value <0.05 and logFC > ±1 as screening criteria, and presented volcano and heatmap of DEG (Figure 2). The results showed that a total of 858 DEGs were identified in the GSE161683 dataset, including 452 up-regulated genes and 406 down regulated genes. In the GSE166388 dataset, 498 genes were upregulated and 429 genes were downregulated. We integrated the DEGs of two datasets and conducted enrichment analysis to clarify the biological functions and pathways of DEGs (Figure 3). BP term in GO, it mainly involves the response to bacteria and viruses and the transmission of cytokine signals; CC term in GO, it mainly involves coronal envelope, secret granule lumen, and cytoplasmic vessel lumen; MF term in GO, it mainly involves oxidoreductase activity and serine type endopeptidase activity. KEGG analysis shows that these DEGs mainly involve Lipoic acid metabolism, IL-17 signaling pathway, and TCA cycle.

Results of WGCNA Analysis

After obtaining DEGs, we conducted WGCNA analysis to further explore the identification of characteristic gene modules in the psoriasis datasets GSE161683 and GSE166388 and to investigate the correlation between gene networks and phenotypes (Figure 4). The results showed that in the GSE161683 dataset, the first value to reach the scale-free topological fitting index (0.8)

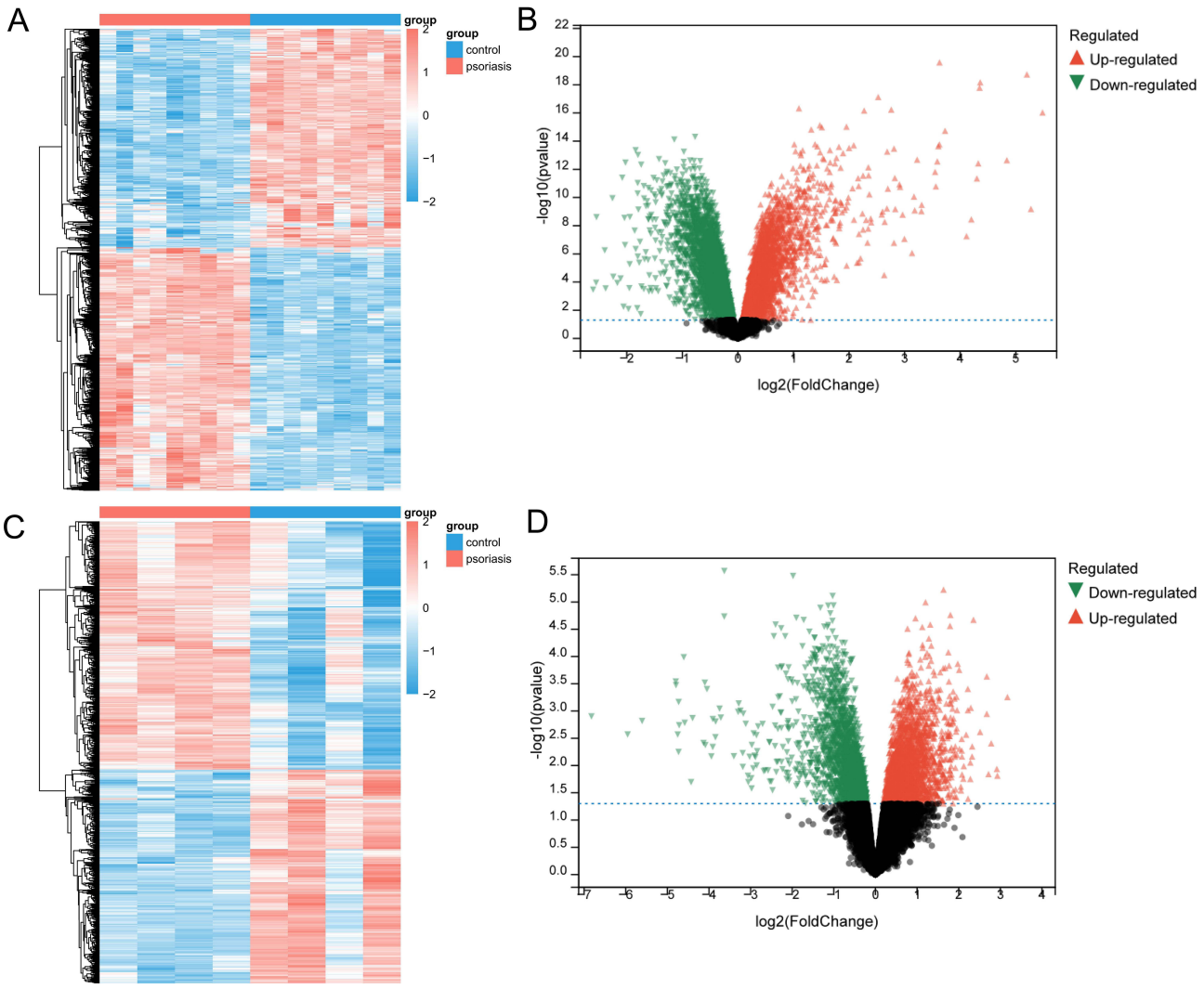

Figure 2 DEGs analysis of GSE161683 and GSE166388. (**A**) DEGs volcano map of GSE161683 dataset; (**B**) DEG heatmap of GSE161683 dataset; (**C**) DEG volcano map of GSE166388 dataset; (**D**) DEG heatmap of GSE166388 dataset.

was 30, therefore the power value was selected as 30 (Figure 4A), and 6 modules were identified, among which the Brown module contains 460 genes and has the highest correlation with module traits (0.98) (Figure 4B and C). In the GSE166388 dataset, the first value to reach the scale-free topological fitting index (0.8) is also 30, so the power value selection is also 30 (Figure 4D), and 11 modules are identified, among which the bisque4 module contains 966 genes and has the highest correlation with module traits (0.90) (Figure 4E and F).

Results of PDCRGs Identification

Subsequently, we intersected the genes contained in the DEGs and Brown, bisque4 modules to obtain core differentially expressed genes (co-DEGs), and identified a total of 168 co DEGs (Figure 5A). After obtaining co-DEGs, we compared them with our self built CRG database and identified a total of 34 psoriasis differential cuproptosis related genes (PDCRGs) (Figure 5C). Compared with healthy controls, these PDCRGs were significantly upregulated in the psoriasis patient dataset (Figure 5B), and there was a significant positive correlation between these PDCRGs (Figure 5D).

Results of PPI Analysis

To further identify the interaction relationships between these 34 PDCRGs, we uploaded them to the STRING database for PPI analysis (Figure 6A–E). The results showed that a total of 34 nodes and 47 edges were obtained, with an average node

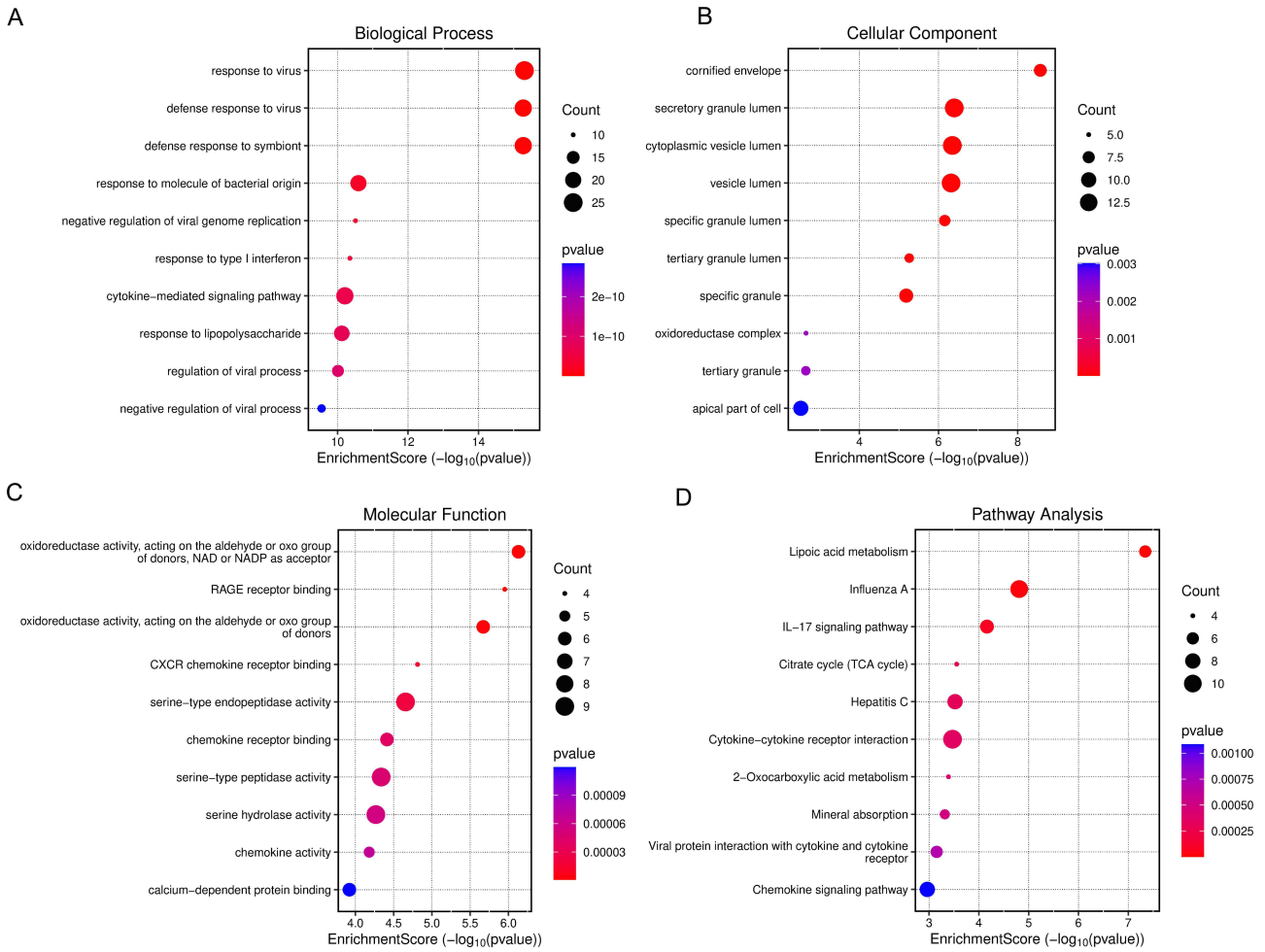

Figure 3 Enrichment analysis of DEGs. (**A**) GO analysis BP term of DEGs; (**B**) GO analysis CC term of DEGs; (**C**) GO analysis MF term of DEGs; (**D**) KEGG analysis of DEG.

degree of 2.76. We selected six Hub genes, including STAT1, DLD, GBP1, CXCL10, LIAS, and PDHB, based on the degree, MCC, Betweenness, and Closeness values of the top 10 ranked by the CytoHubba algorithm. Subsequently, we predicted the regulatory relationships between transcription factors and miRNAs related to six Hub genes based on TRRUST, miRArbase, and Mirwalk. However, we only found that STAT1 and CXCL10 each had six regulatory factors. By integrating the intersection results of miRArbase and Mirwalk, we found that the six Hub genes matched a total of 59 miRNAs (Figure 6F).

Results of PDCRG Enrichment Analysis

We further explored the biological functions and pathways of PDCRGs through GO and KEGG analysis. GO analysis identified 37 terms (Figure 7A), among which BP mainly includes copper ion import, tricarboxylic acid cycle, and glucose metabolic process; CC mainly includes pyrovate dehydrogenase complex, early endosome membrane, and mitochondrion; MF mainly includes pyravate dehydrogenase activity, copper ion binding, and copper ion transmembrane transporter activity. And KEGG analysis obtained a total of 22 signaling pathways, mainly including citrate cycle, pyruvite metabolism, and glycolysis/gluconeogenesis (Figure 7B). Meanwhile, we also annotated 17 signaling pathways of 6 Hub genes (Figure 7C).

Results of PDCRG Machine Learning Analysis

In this study, we applied three machine learning methods RF, SVM, and LASSO-COX to identify key diagnostic biomarkers of PDCRGs and reveal the biological significance of cuproptosis in psoriasis. The results show that the top

https://doi.org/10.2147/JIR.S569453

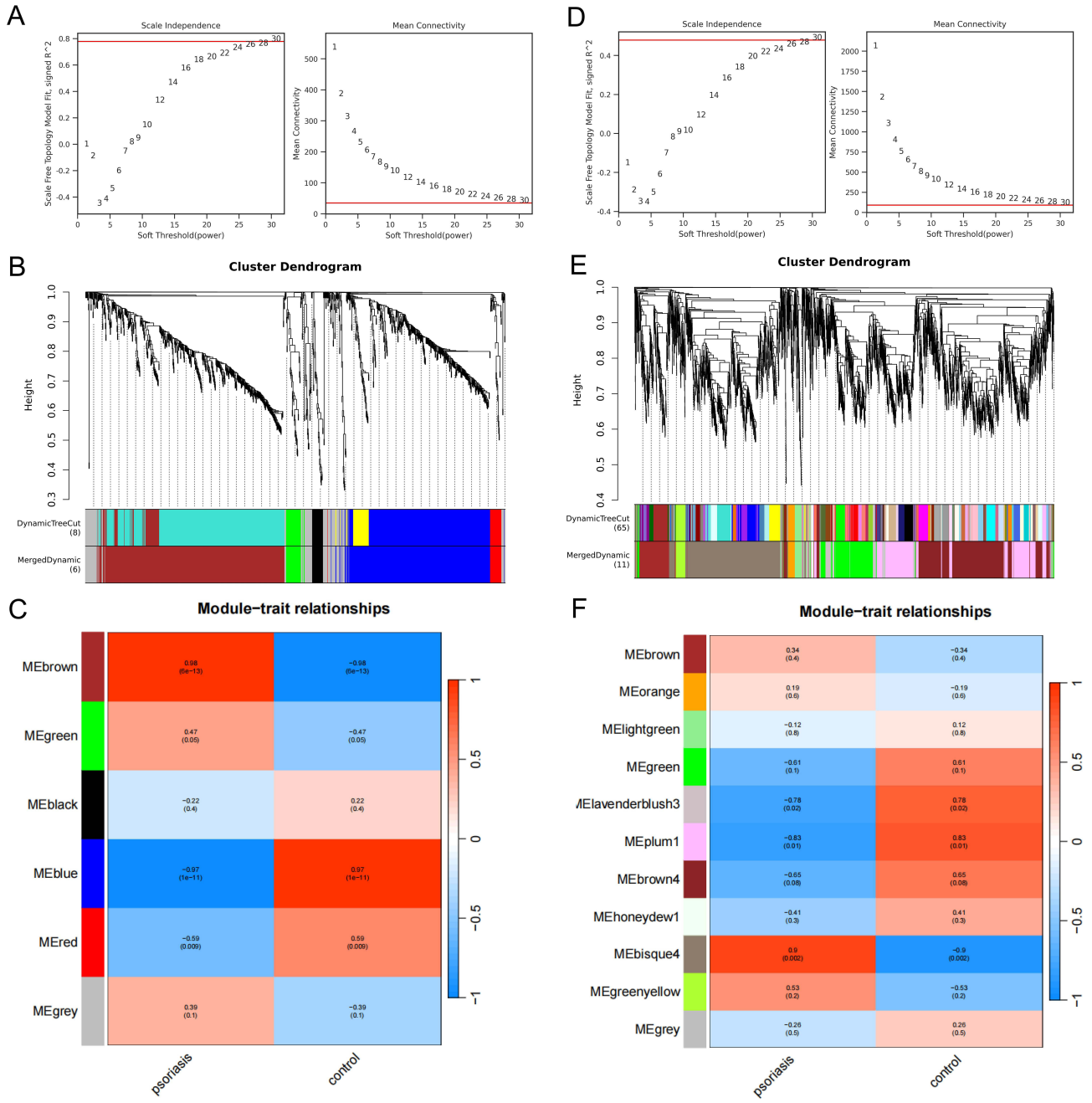

Figure 4 WGCNA analysis. (**A**) The power value of the GSE161683 dataset is 30; (**B**) Based on the selected power values, a weighted co expression network model was established, and 1045 genes were ultimately divided into 6 modules; (**C**) Using Pearson correlation algorithm to calculate the correlation coefficient and p-value between module feature genes and traits, with the MEbrown module showing the highest correlation; (**D**) The power value of the GSE166388 dataset is also 30; (**E**) Based on the selected power values, a weighted co expression network model was established, and 3904 genes were ultimately divided into 11 modules; (**F**) Using Pearson correlation algorithm to calculate the correlation coefficient and pValue between module feature genes and traits, among which bisque4 module has the highest correlation.

10 key PDCRGS screened out in RF include APOL6, CD274, VNN1, LIPT1, TYMP CXCL10, TCN1, PLAT, LIAS and AKR1B10 (Figure 8A); Four key PDCRGS were screened out in LASSO-COX, including APOL6, ATP7B, LIAS and CD274 (Figure 8B); In SVM, a total of 5 key PDCRGs were selected, including APOL6, LIAS, CD274, MTF1, and LIPT1 (Figure 8C). We synthesized the results obtained from three machine learning methods and ultimately identified three key PDCRGs, namely APOL6, CD274, and LIAS (Figure 8D). Moreover, the expression levels of these three PDCRGs were significantly elevated in the psoriasis patient dataset (Figure 8E).

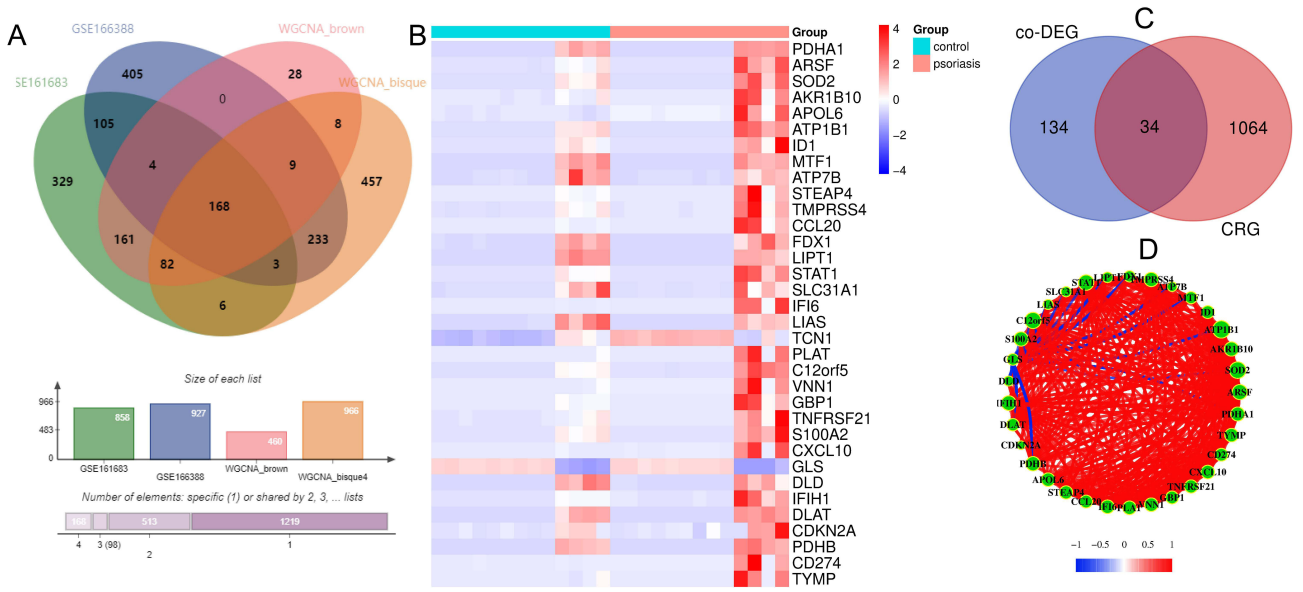

Figure 5 Identification of co-DEG and PDCRGs. (**A**) A total of 168 co-DEGs were identified through DEGs and WGCNA analysis in two psoriasis datasets; (**B**) The expression of 34 PDCRGs in the psoriasis dataset; (**C**) 34 PDCRGs were selected from CRGs and co DEGs; (**D**) Correlation analysis among 34 PDCRGs, with red indicating positive correlation and blue indicating negative correlation.

Results of ssGSEA and ROC Analysis

To further investigate the pathways involved in APOL6, CD274, and LIAS in the psoriasis dataset, we conducted ssGSEA analysis on these three key PDCRGs. The results showed that APOL6 in the key PDCRG mainly involves 16 signaling pathways (Figure 9A), among which the calcium signaling pathway has the highest significance (P = 0.0041); CD274 mainly involves 12 signaling pathways (Figure 9B), among which long term latency has the highest significance (P = 0.0491); LIAS mainly involves 4 signaling pathways (Figure 9C), among which inositol phosphate metabolism (P = 0.0078). To clarify whether the three key PDCRGs have predictive diagnostic significance for AD, an external dataset GSE277173 was used for ROC analysis of APOL6, CD274, and LIAS to determine the accuracy of these key PDCRGs as psoriasis disease characteristic genes. By calculating the area under the ROC curve (AUC), the closer the AUC value is to 1, the better the predictive performance. The results showed that the expression of APOL6, CD274, and LIAS was significantly increased in the GSE277173 dataset compared to the control group. The AUC values of APOL6, CD274, and LIAS were 0.66, 0.67 and 0.90, respectively (Figure 9D–F), indicating that APOL6, CD274, and LIAS can serve as diagnostic markers for copper metabolism disorders in psoriasis.

Results of Immune Infiltration Analysis

We conducted in-depth analysis of 34 PDCRGs expression matrices using CIBERSORT, aiming to accurately quantify the abundance and spatial distribution characteristics of various immune cells in psoriasis patient samples, and provide key evidence for revealing their intrinsic relationship with treatment response biomarkers. The results showed that compared with healthy patient samples, the expression of Mast cells activated and T cells CD4 memory resting in psoriasis patient samples was significantly reduced. Although there was an increasing trend in dendritic cell activated, there was no difference (Figure 10A and C). There is a significant positive correlation between γδ T cell monocytes, and NK cell resting, while there is a significant negative correlation between plasma cells, T cells follicular helper and T cell CD4 memory resting (Figure 10B). In addition, we also found that compared with normal healthy samples, the proportion of T cells and B cells in psoriasis patient samples increased (Figure 10D).

Results of Skin Lesions Characteristics in Psoriasis Model Mice

During the modeling period of each group of mice, there was no significant change in skin lesions in mice treated with Vaseline cream, while mice treated with imiquimod cream showed obvious red rashes and bleeding spots on their skin, accompanied by

https://doi.org/10.2147/JIR.S569453

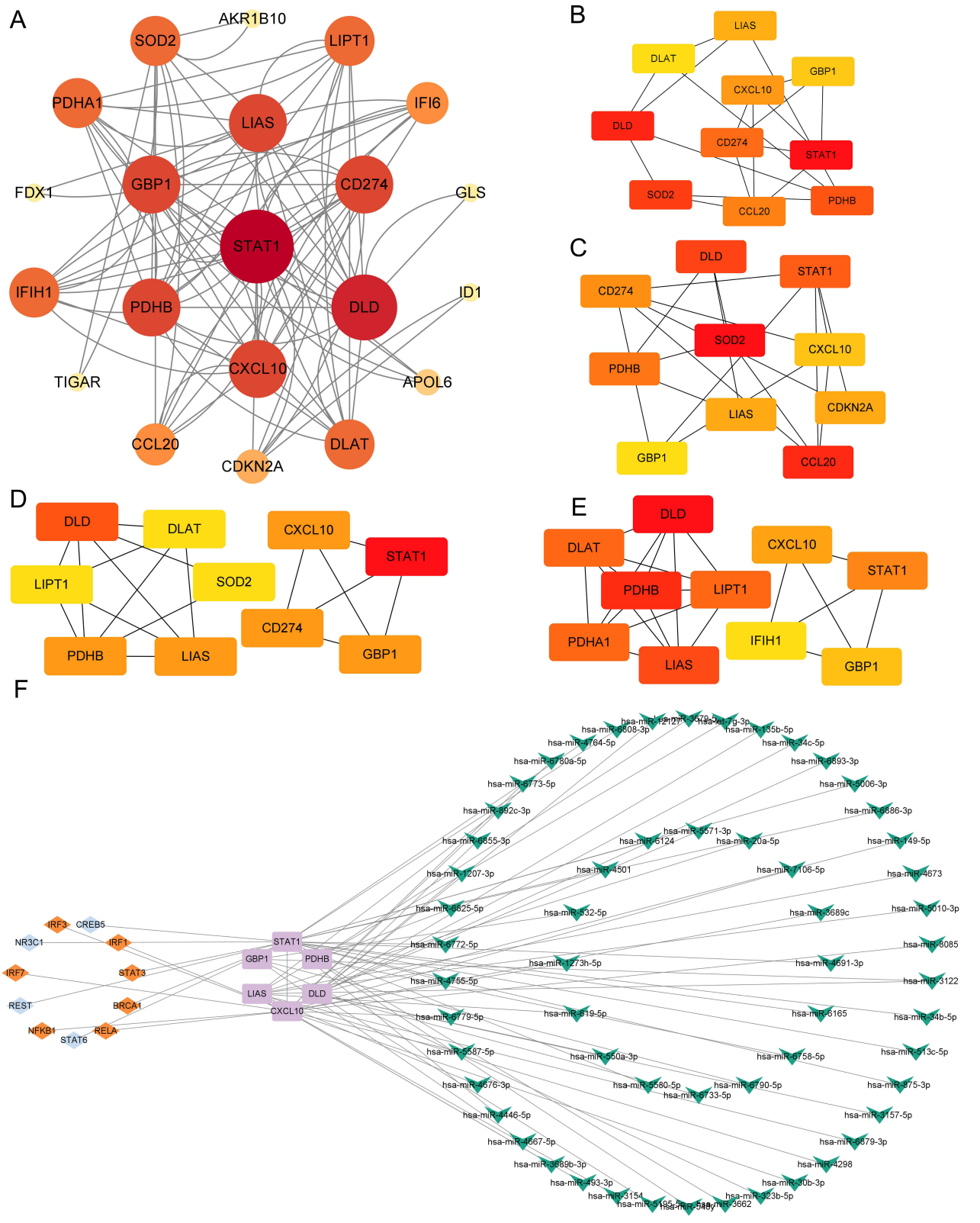

Figure 6 PPI analysis. (**A**) PPI plot of 34 PDCRGs after removing free nodes; (**B**) MCC analysis based on cytohubba algorithm; (**C**) Degree analysis based on CytoHubba algorithm; (**D**) Closeness analysis based on CytoHubba algorithm; (**E**) Betweenness analysis based on the CytoHubba algorithm; (**F**) The "TF mRNA miRNA" network of 6 Hub genes. The purple modules represent hub genes, the green modules represent mirnas, the Orange modules represent activating transcription factors, and the blue ones represent inhibitory transcription factors.

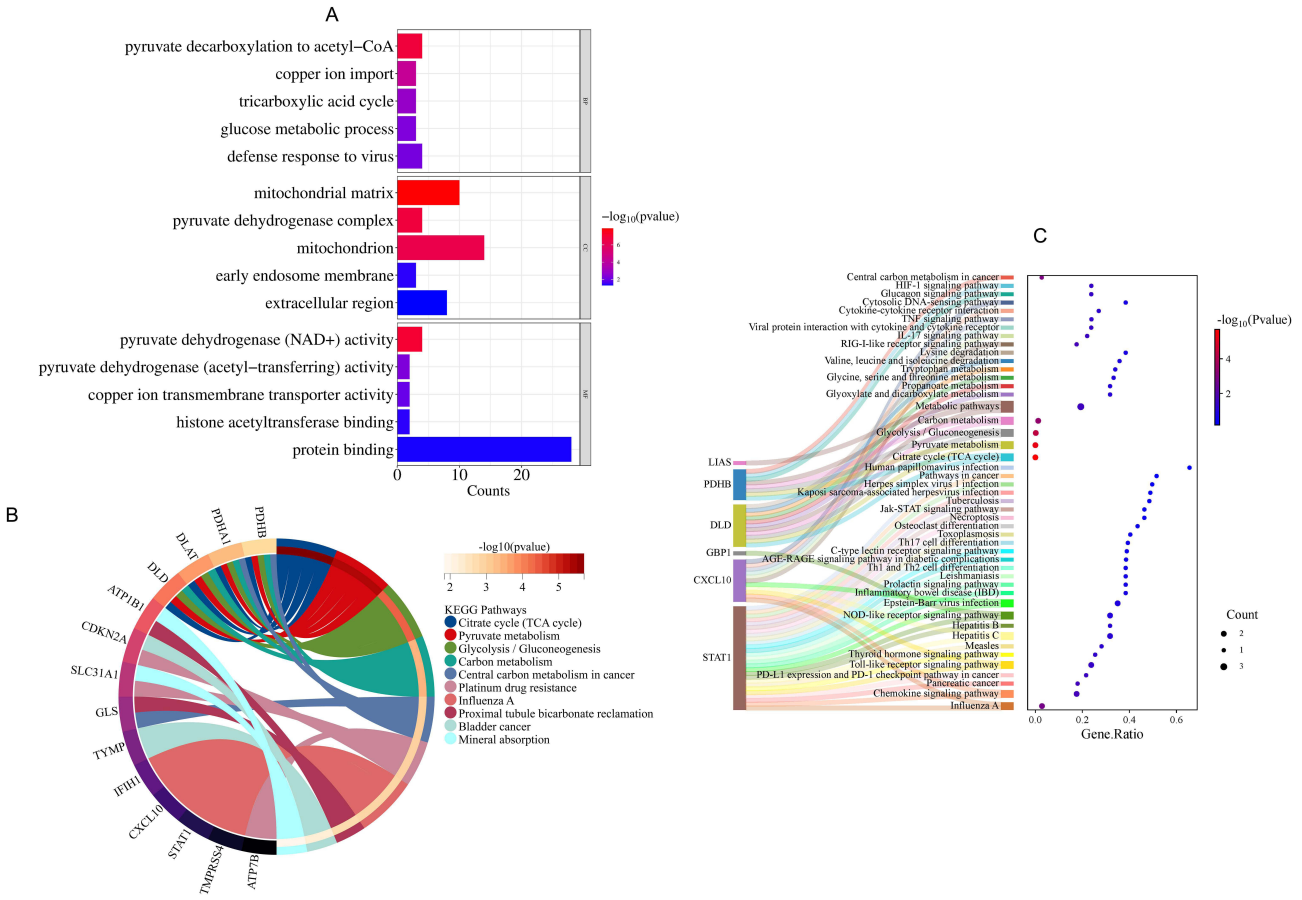

Figure 7 Enrichment analysis of PDCRGs. (**A**) GO analysis of PDCRGs; (**B**) KEGG analysis of PDCRGs; (**C**) Sankey diagram of 6 Hub gene related pathways.

patchy and continuous silver white scales. In addition, we evaluated the severity of psoriasis in mice using the MPAS. The results showed that compared with the Sham group mice, the MPASI score of the psoriasis group mice was significantly increased (Figure 11A and C), which not only indicates that we have successfully constructed a psoriasis animal model but also demonstrates the changes in skin lesions of the psoriasis model mice. In addition, psoriasis is an inflammatory skin disease characterized by the appearance of red patches on the skin surface accompanied by the production of silver white flakes. Therefore, we observed the general pathological morphology of each group of mice through HE staining (Figure 11B). The results showed that the epidermis of Sham group mice did not thicken, and the skin morphology and structure were intact and clear. Compared with the Sham group mice, the psoriasis group mice showed thickening of the epithelial layer, local dilation of capillaries in the superficial dermis, obvious focal hyperkeratosis, prolonged and undulating skin processes, and extensive infiltration of inflammatory cells in the deep dermis.

Results of Copper Levels in Psoriasis Model Mice

SLC31A1 is a key transporter for Cu to be transported into cells. In order to further observe the changes of the inward uptake characteristic marker SLC31A1 of Cu in psoriasis model mice, we detected the expression of SLC31A1 in the skin tissue of each group of mice and the copper ion level in the serum through IHC. The results showed that compared with the Sham group, the expression level of SLC31A1 in the skin tissue of psoriasis group mice was significantly increased (Figure 12A). In addition, we also found a significant increase in Cu levels in the serum of psoriasis group mice, while Sham group mice did not show this change (Figure 12B).

https://doi.org/10.2147/JIR.S569453

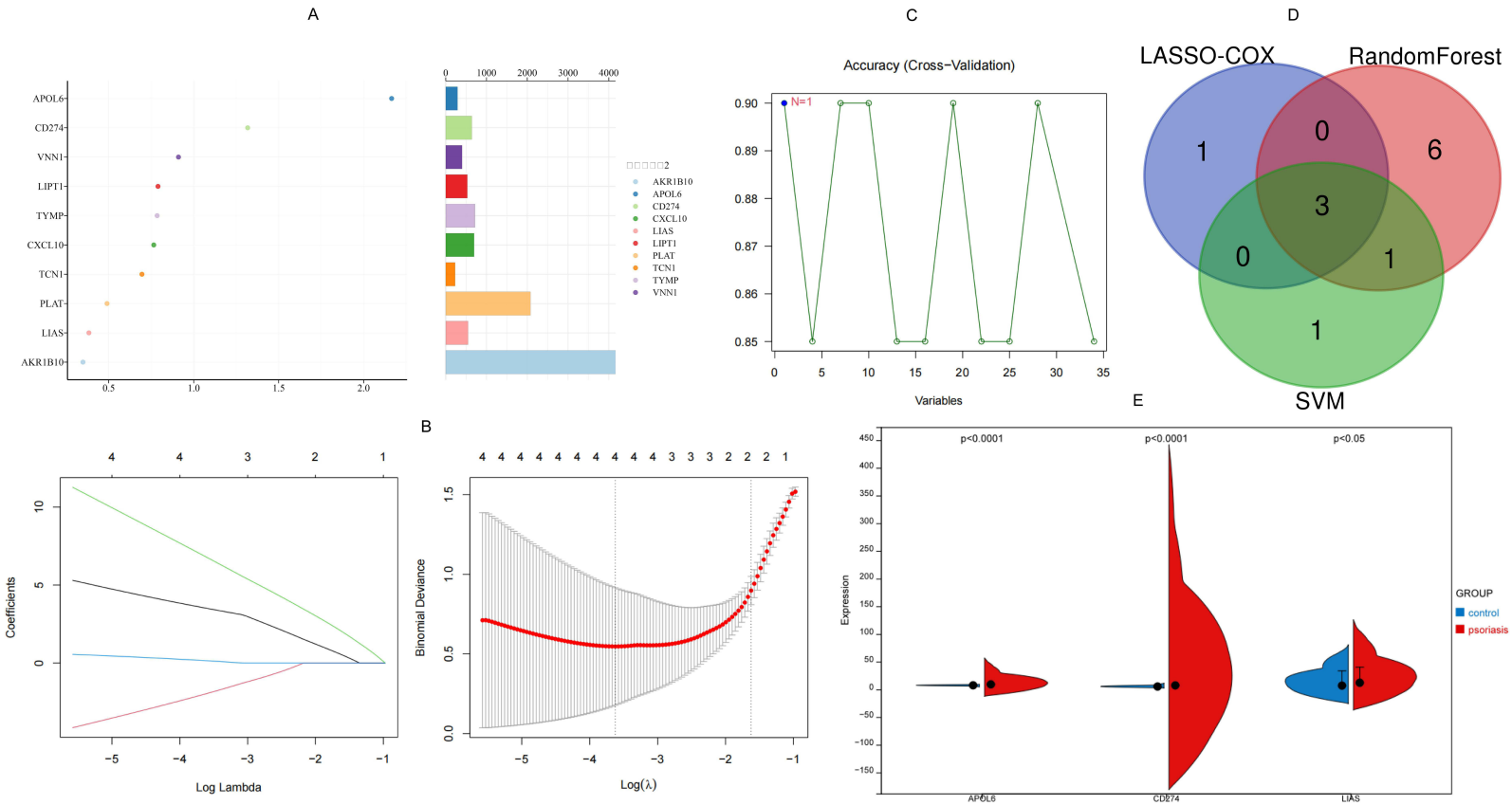

Figure 8 Machine learning. (**A**) selects the top 10 PDCRGs in RF analysis; (**B**) Four PDCRGs were selected in Lasso Cox analysis; (**C**) Select 5 PDCRGs in SVM analysis; (**D**) Three machine learning analysis methods have identified three key PDCRGs, including APOL6, CD274, and LIAS; (**E**) The expression of three key PDCRGs in the psoriasis dataset.

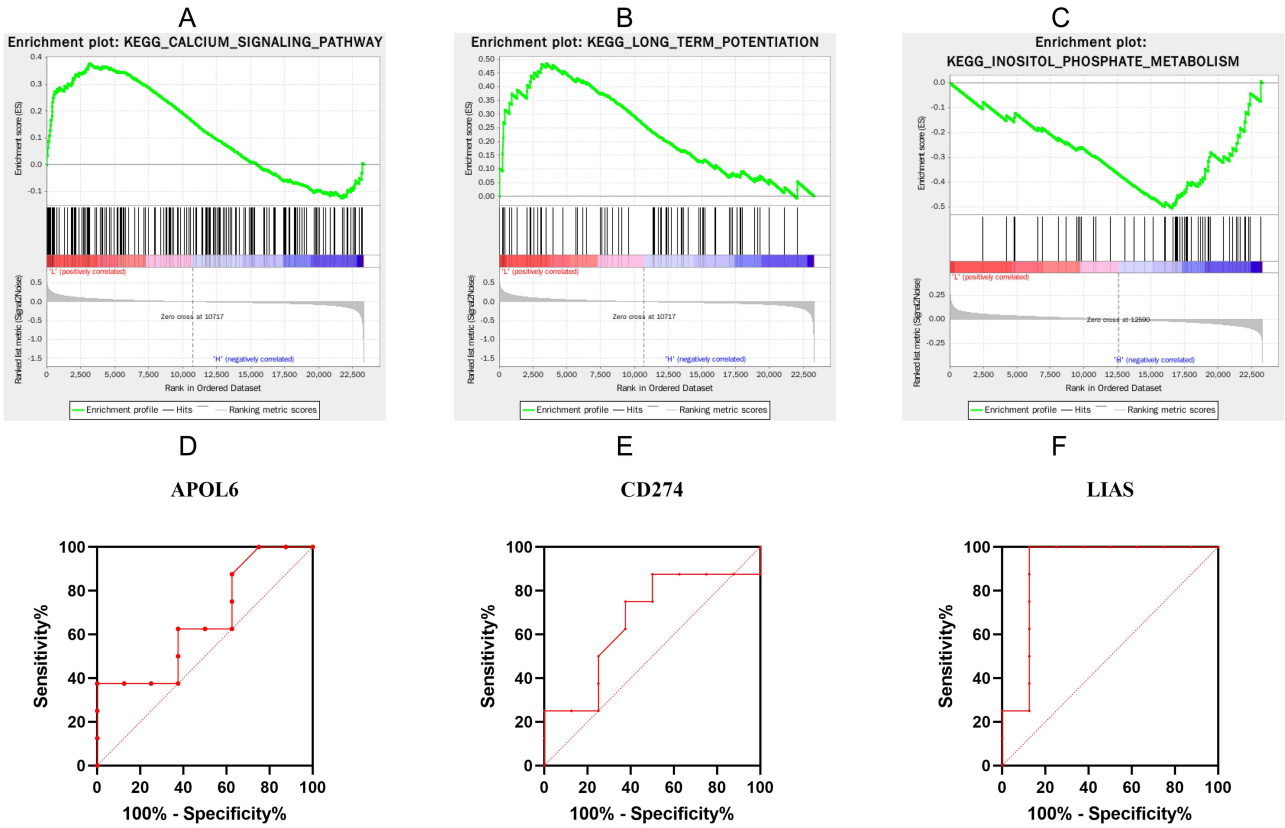

Figure 9 Identification of GSEA and ROC. (**A**) The GSEA analysis of APOL6 showed that the calcium signaling pathway had the highest significance; (**B**) The GSEA analysis of CD274 showed the highest significance for long term potential; (**C**) The GSEA analysis of LIAS showed that inositol phosphate metabolism had the highest significance; (**D–F**) ROC analysis of APOL6, CD274, and LIAS.

Results of Inflammation and Oxidative Stress Levels

An increase in copper ion levels can directly induce cuproptosis and catalyze the Fenton reaction, leading to an increase in oxidative stress levels, which then activates cellular inflammatory factors to promote the occurrence of inflammatory reactions. Therefore, we also measured the levels of inflammation and oxidative stress in the serum of each group of mice. The results showed that compared with the Sham group mice, the levels of inflammatory factors IL-1β, IL-6, IL17, and IL23 in the serum of psoriasis group mice were significantly increased, and the levels of ROS and MDA were also significantly increased, while the levels of SOD and GSH-Px were significantly decreased (Figure 13A–H). This indicates that high levels of copper ions not only mediate cuproptosis but also promote an increase in oxidative stress and inflammation levels. To further investigate the effect of cuproptosis on inflammatory infiltration in psoriasis, we also observed the expression of ATP7B, FDX1 and NF-κB. The results showed that compared with the blank group, the expression level of ATP7B in psoriasis group mice was significantly reduced (Figure 13I), and the activation of FDX1 significantly enhanced the expression of NF-κB, indicating that high levels of copper aggregation can promote the increase of inflammation levels.

The Results of Changes in PDRGs and TCA Cycle Pathways in Psoriasis

In bioinformatics, we screened 6 Hub genes and 3 key PDCRGs, and therefore detected the gene expression levels in the skin tissue of psoriasis model mice. The results showed that compared with the Sham group, the expression of STAT1, DLD, GBP1, CXCL10, PDHB, APOL6, CD274 and LIAS mRNA in the skin tissue of psoriasis group mice was significantly increased. In addition, we also detected the protein expression of key PDCRGs, and similarly, the expression of APOL6, CD274, and LIAS proteins was significantly increased in the skin tissue of psoriasis model mice (Figure 14). It is worth noting that the enrichment analysis results indicate that these PDCRGs mainly involve the TCA cycle, and

https://doi.org/10.2147/JIR.S569453

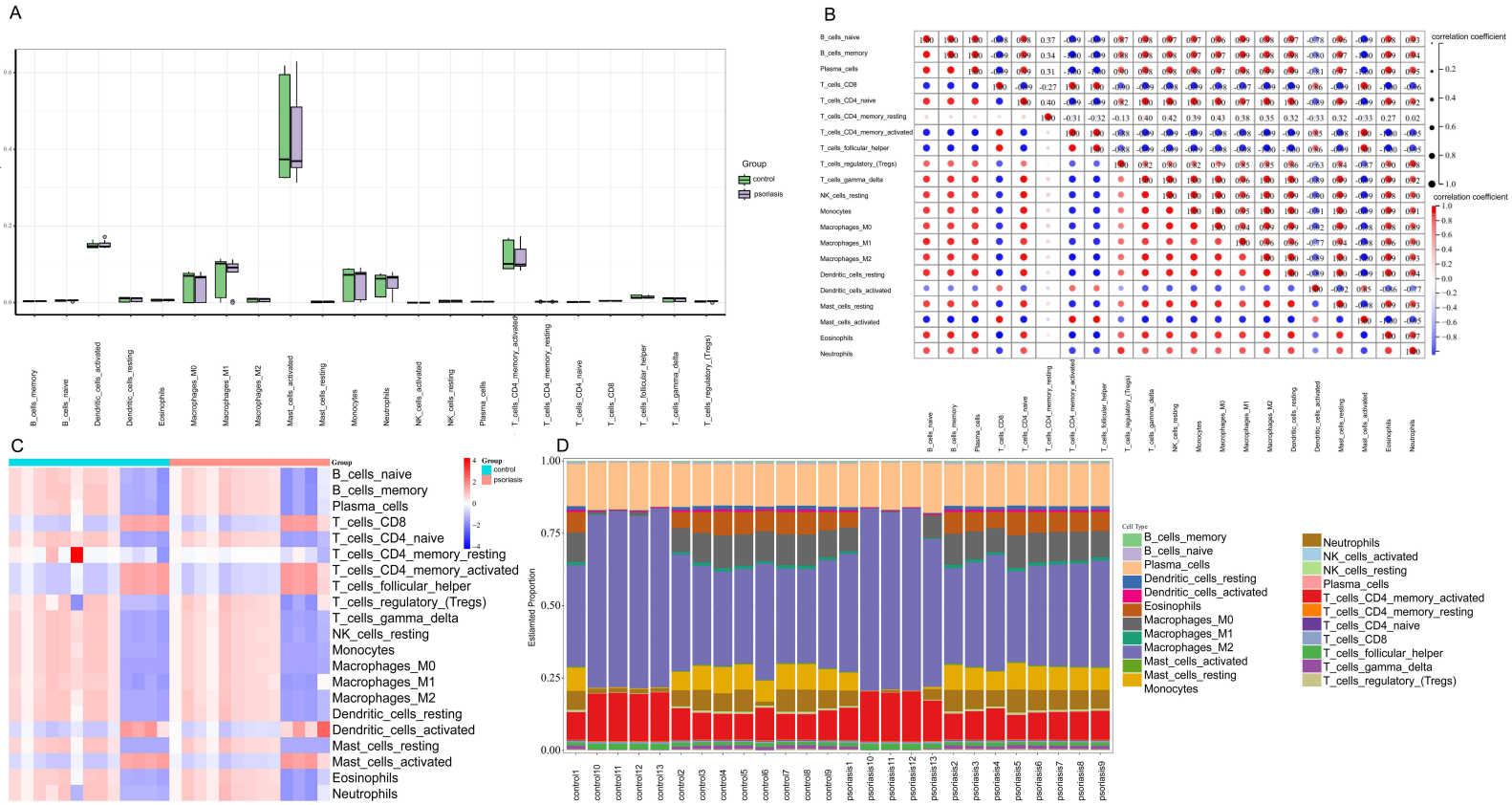

Figure 10 Immune infiltration analysis. (**A**) Expression of 22 immune cells in psoriasis patients and normal healthy individuals; (**B**) Correlation of 22 types of immune cells; (**C**) Cluster heatmap of 22 immune cells in the psoriasis dataset for each sample; (**D**) The proportion of 22 immune cells in each sample of the psoriasis dataset.

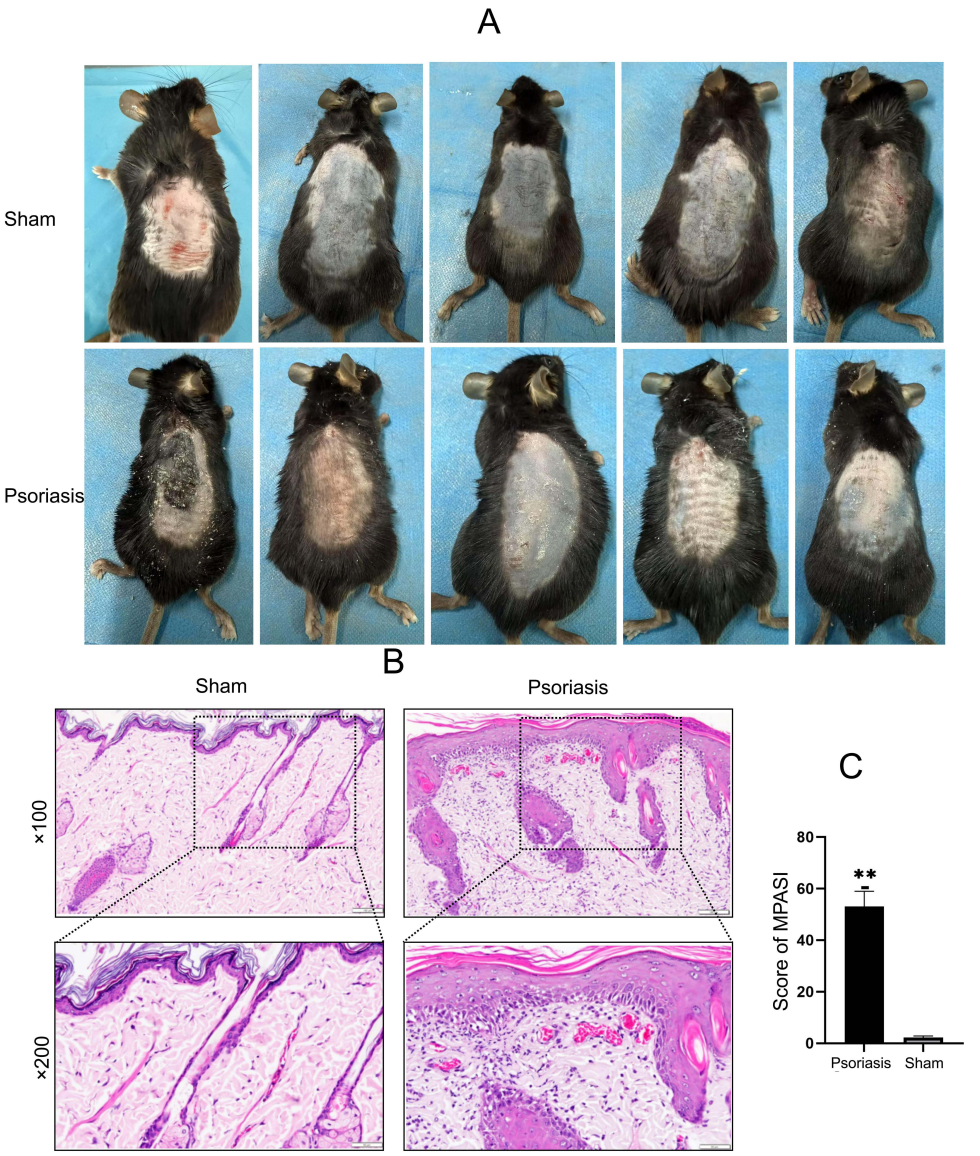

Figure 11 Construction of Psoriasis Model. (**A**) A psoriasis model was constructed by applying IMQ to the back of mice for one week; (**B**) HE staining of skin tissues in Sham group and psoriasis group mice; (**C**) The MPASI scores of Sham group and psoriasis group mice, n = 5, compared with the Sham group, **P < 0.01.

TCA cycle disorders can lead to mitochondrial dysfunction, promote Cu deposition, and cause programmed cell death. Therefore, we also detected the protein expression levels of PDCRGs related to the TCA cycle, including DLD, DLAT, and PDHB. The results confirmed our hypothesis, and we found that the protein expression levels of DLD, DLAT, and PDHB were significantly increased in IMQ induced psoriasis model mice. This indicates a direct interaction between Cu deposition and TCA cycle.

Discussion

Psoriasis, as a chronic inflammatory skin disease driven by genetic susceptibility, immune dysfunction, and environmental factors, not only causes persistent itching, pain, and joint damage but also has a profound impact on the social, psychological, and quality of life of patients. The high medical costs, loss of labor capacity, and burden of comorbidities pose significant socio-economic challenges.[31] The immune inflammatory cascade reaction in psoriasis is the core driving factor, which not only directly stimulates excessive proliferation and abnormal differentiation of keratinocytes but also forms a vicious cycle through epigenetic regulation and the cGAS/STING pathway, leading to local oxidative stress

https://doi.org/10.2147/JIR.S569453

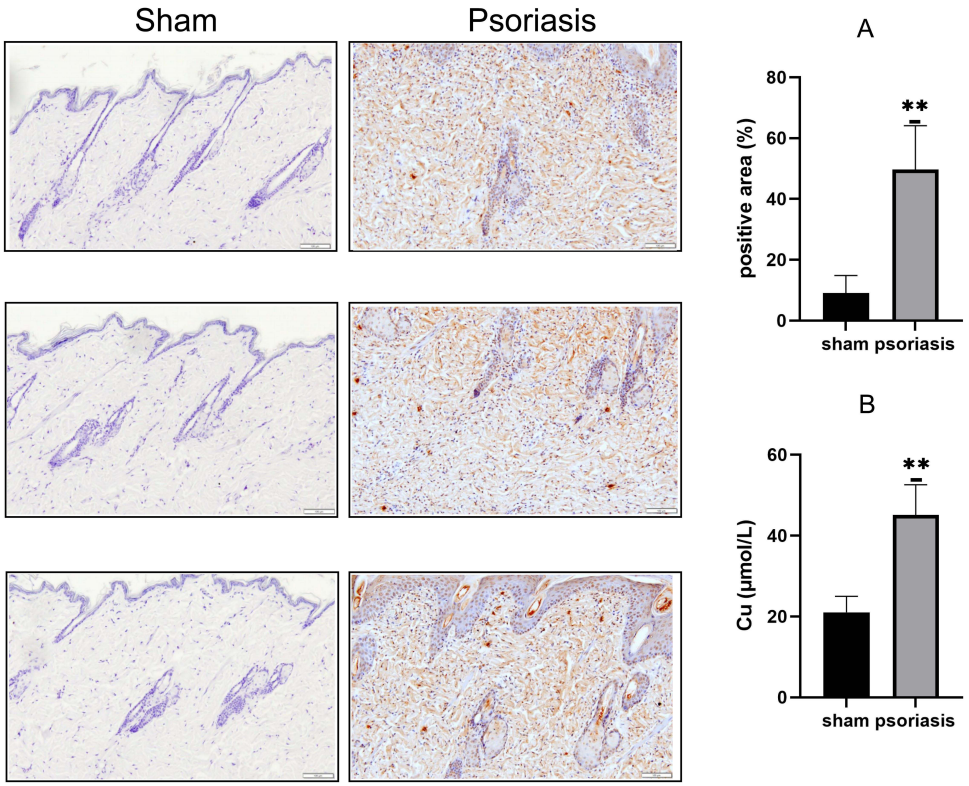

Figure 12 Copper content levels in psoriasis model. (**A**) The positive expression of SLC31A1 was significantly increased in the skin tissue of psoriasis model mice, ×100, n = 3, compared with the Sham group, **P < 0.01; (**B**) The level of Cu significantly increased in the serum of psoriasis model mice, n = 3, compared with the Sham group, **P < 0.01.

outbreaks and mitochondrial dysfunction.[32] It is worth noting that this study found that the imbalance of copper metabolism homeostasis plays a key role in the pathological network of psoriasis. Copper, as a core cofactor of various oxidoreductases, can accumulate in cells (copper overload) and catalyze the generation of reactive oxygen species (ROS) through the Fenton reaction, directly inducing lipid peroxidation, DNA damage, and mitochondrial membrane potential collapse, activating a new form of cell death-cuprotosis.[33,34] The synergistic abnormal expression of cuprotosis related genes APOL6, LIAS, and CD274 identified in psoriasis lesions suggests that the cuprotosis pathway may be a key molecular bridge connecting copper metabolism disorders, oxidative damage, and chronic inflammation in psoriasis.

We conducted DEGs and WGCNA analysis on two psoriasis datasets, GSE161683 and GSE166388, and identified 168 co-DEGs in psoriasis. Subsequently, we compared them with a self built cuproptosis database and identified a total of 34 PDCRGs. Through PPI analysis, we identified 6 Hub genes from 34 PDCRGs, including STAT1, DLD, GBP1, CXCL10, LIAS, and PDHB. In addition, we obtained three key PDCRGs through machine learning analysis, namely APOL6, CD274, and LIAS. Eight core PDCRGs (STAT1, DLD, GBP1, CXCL10, CD274, APOL6, LIAS, PDHB) synergistically drive the pathological process of psoriasis. Existing research has found that STAT1 (a signal transduction protein containing the SH2 domain) activated by the inflammatory microenvironment enters the nucleus through Tyr701 phosphorylated dimer, directly upregulating the copper transporter SLC31A1, leading to copper ion overload in keratinocytes.[35] The influx of copper ions into mitochondria triggers a toxic reaction in DLD, where the flavin binding domain of the E3 component of the PDH complex generates ROS during the reduction of Cu^2+, inducing abnormal aggregation of thiocyanate proteins represented by DLAT.[36] At the same time, copper ions disrupt the stability of the [4Fe-4S] cluster of LIAS,[37] inhibit the synthesis of new lipoic acid, and weaken antioxidant defense. The dysfunction of PDHB forces pyruvate to shift towards lactate production, and the triple effect together forms a “thiocyanate crisis”, ultimately leading to FDX1 dependent cuprotosis.[38] The mitochondrial breakdown releases DAMPs such as mtDNA, which activate STAT1 secondary phosphorylation through TLR9/P2X7 receptors, thereby initiating an inflammatory

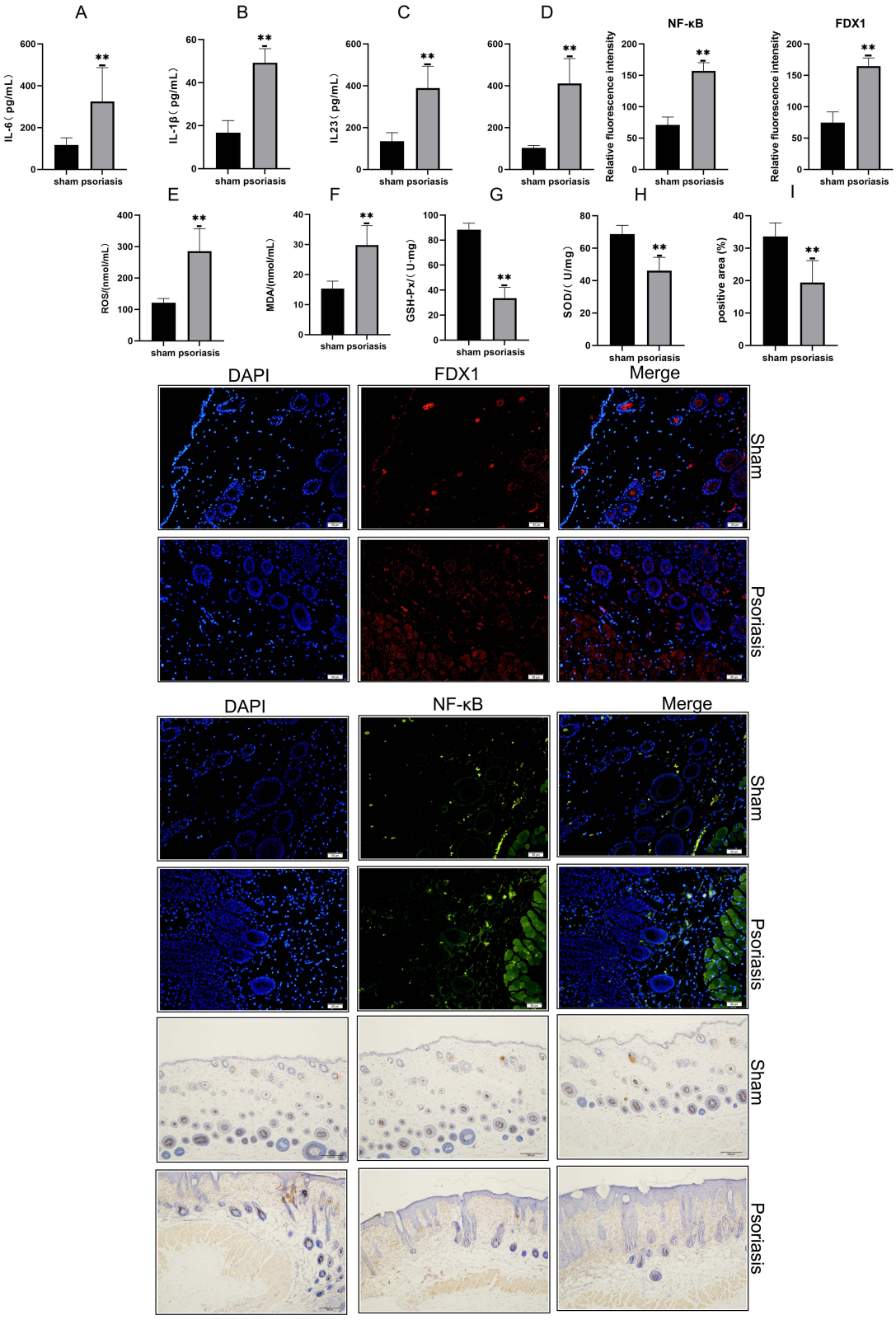

Figure 13 Detection of Inflammation and Oxidative Stress Levels in Psoriasis Model. (**A**–**D**) Expression of Inflammatory Factors IL-1 β, IL-6, IL17, and IL23 in the Serum of Mice in Each Group, n = 5, compared with the Sham group, **P < 0.01; (**E**–**H**) The expression of oxidative stress factors ROS, MDA, SOD, and GSH-Px in the serum of mice in each group was n = 5, and compared with the Sham group, *P < 0.05, **P < 0.01; (**I**) Detection of ATP7B expression levels in skin tissues of mice in each group, ×100, n = 3, compared with the Sham group, **P < 0.01.

https://doi.org/10.2147/JIR.S569453

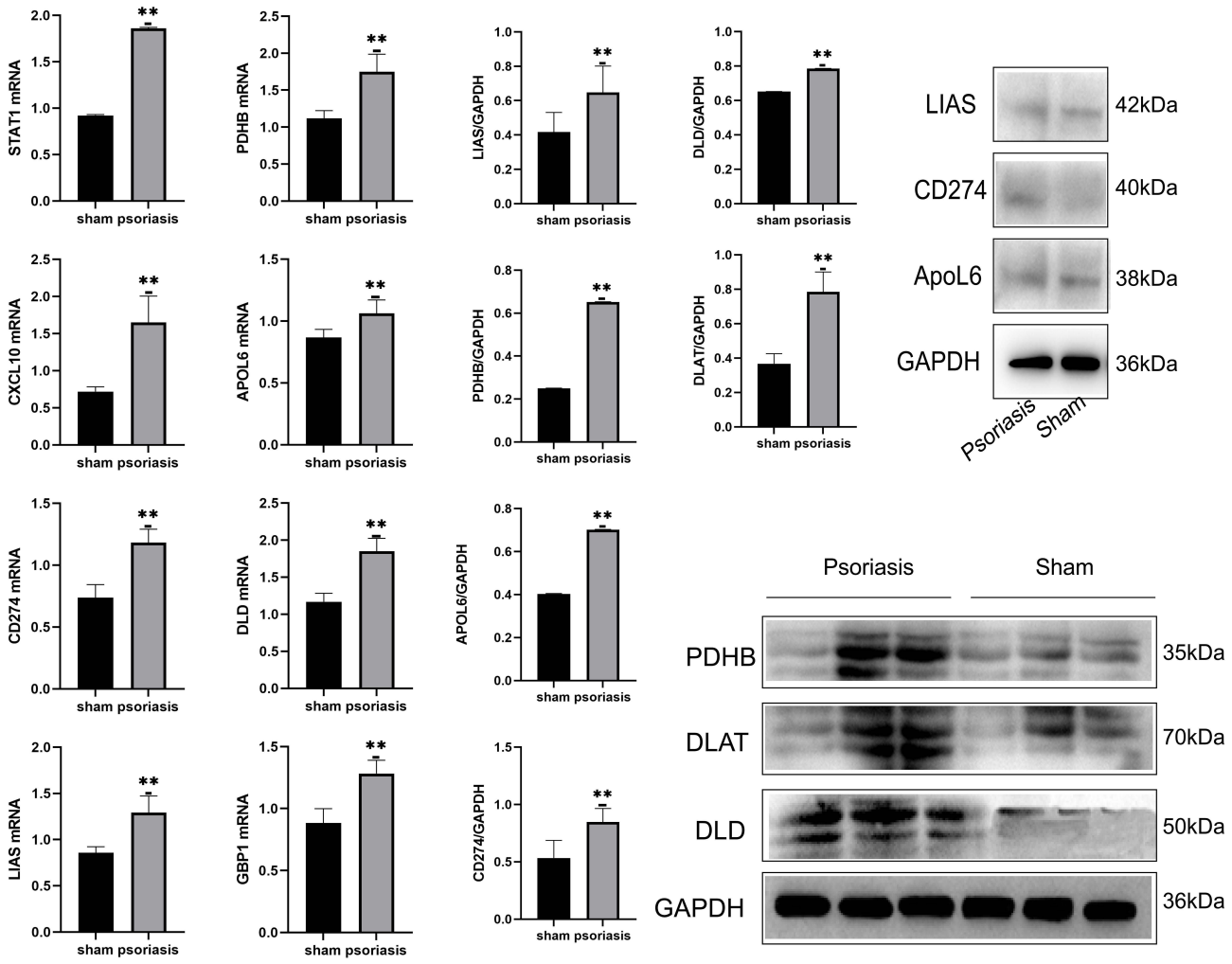

Figure 14 PDCRGs and TCA cycle pathway related mRNA, protein expression. n = 3, compared with Sham group, *P < 0.05, **P < 0.01.

cascade reaction. Phosphorylated STAT1 induces high expression of CXCL10, which breaks through the classical pathway of CXCR3 and directly binds to the CD14 receptor of macrophages, activating the PI3K/AKT-IKK axis to drive NF-κB into the nucleus and upregulating TNF-α/IL-23 expression.[39] On the other hand, upregulating GBP1 recruits p62 protein from its C-terminal α helix domain to clear damaged mitochondria, releasing mtROS that drives macrophages to polarize towards the IFN-γ phenotype, forming an amplification loop called "CXCL10-GBP1-Microcytes".[40] Based on the existing research results, we speculate that the potential mechanism by which copper death promotes psoriasis may be by inhibiting the clearance of immune cells. Chronic inflammation locks in the pathological state of psoriasis through a dual mechanism. TNF-α activates STAT3 through JAK2, and its DNA binding domain binds to the CD274 promoter, causing keratinocytes to overexpress CD274. It then binds to T cell CD274 receptors through the immunoglobulin V-like domain, inhibiting CD8+ T cell clearance of cuprotosis cells.[41] APOL6 anchors lipid droplets through the C-terminal domain and binds to perilipin 1, blocking HSL lipase activity and inhibiting lipolysis, forcing cells to rely on glycolysis. The lactate accumulation caused by PDHB dysregulation activates macrophage HIF-1α, followed by upregulation of TNF-α expression, promoting inflammatory response and leading to core lesions such as epidermal barrier disruption, inflammatory infiltration, and immune microenvironment imbalance.[42–45]

In addition, we found through enrichment analysis that these PDCRGs are mainly related to TCA cycle. Eight cuprotosis core genes (STAT1, DLD, GBP1, CXCL10, CD274, APOL6, LIAS, PDHB) in psoriasis cascade interfere with the TCA cycle, triggering copper dependent cell death and driving chronic inflammation. Among them, DLD, PDHB and LIAS, as key components of the TCA cycle, directly affect mitochondrial metabolic homeostasis by regulating the

function of pyruvate dehydrogenase complex (PDHc) and protein lipoylation.[46,47] Existing research has found that PDHB catalyzes the conversion of pyruvate to acetyl-CoA and initiates the TCA cycle. LIAS mediated lipoylation modification is the basis for the function of PDHc core proteins (such as DLAT), while DLD maintains the integrity of the electron transport chain.[48,49] When the above genes are expressed abnormally, TCA cycle disruption makes it easier for thiolated proteins to be targeted by accumulated copper ions in mitochondria, inducing abnormal oligomerization and aggregation of DLAT, disrupting the stability of Fe-S cluster proteins, and triggering cuprotosis. TCA cycle collapse triggers three secondary effects of cuprotosis. Firstly, the stress caused by protein toxicity. DLAT aggregation blocks the mitochondrial matrix, leading to LIAS instability and disrupting electron transfer.[50] Secondly, there is an imbalance in energy metabolism. The shortage of acetyl-CoA leads to a sharp decline in ATP synthesis.[51] Finally, there is an increase in oxidative stress. The synergistic activation of Fenton reaction by DLD induced ROS burst and LIAS deficiency induced antioxidant defense deficiency-Cu+ converts H_2O_2 into hydroxyl radicals while consuming GSH, inducing irreversible oxidative damage.[52] Subsequently, cuprotosis further drives the pathological process of psoriasis. On the one hand, dead cells release damaging molecules to activate STAT1 signaling. STAT1 serves as an inflammatory signaling hub, and its SH2 domain mediated JAK/STAT pathway activates the upregulation of copper transporter SLC31A1, promoting excessive copper ion influx into mitochondria;[53] FDX1 in mitochondria reduces Cu^2+ to highly toxic Cu+, which directly targets the lipoylation proteins in the TCA cycle, especially the key reaction catalyzed by DLD.[54] Upregulated chemokine CXCL10 and interferon responsive GBP1 are highly expressed, recruiting inflammatory cell infiltration and promoting excessive proliferation and angiogenesis of keratinocytes.[55] On the other hand, copper ions directly stabilize the expression of immune checkpoint CD274 protein, exacerbating immune escape by inhibiting T cell function. In addition, the psoriasis microenvironment accelerates copper accumulation, and inflammatory factors such as IL-17 upregulate the expression of copper transporter SLC31A1, leading to local copper overload. APOL6 may amplify this process by responding to mitochondrial stress, forcing the epidermis into a vicious cycle of "oxidative damage, abnormal repair and chronic proliferation", manifested as excessive proliferation of keratinocytes, abnormal proliferation of dermal blood vessels, and inflammatory infiltration dominated by macrophages.[56]

We used a MIQ-induced psoriasis mice model to verify our bioinformatics results. The most prominent advantage of this model lies in its ability to rapidly and efficiently reproduce multiple core clinical and immunopathological features of psoriasis, and it demonstrates significant advantages and high universality in terms of operational feasibility and research application value. Our research results showed that in the skin tissue of MIQ induced psoriasis model mice, the mRNA expression of STAT1, DLD, GBP1, CXCL10, CD274, APOL6, LIAS and PDHB was significantly increased, as well as the expression of key PDCRGs proteins APOL6, CD274 and LIAS. We also found high expression of inflammatory factors IL-6, IL1β, IL-17, IL-23, and Cu, accompanied by dysregulation of oxidative stress, manifested as high levels of ROS, MDA, and decreased SOD and GSH-Px. In addition, we also observed abnormal changes in copper transporters ATP7B and SLC31A1, which led to excessive accumulation of copper. The expression of cuprotosis marker protein FDX1 was significantly increased, and FDX1 promoted NF-κB activation. It is worth noting that the expression of TCA cycle related proteins DLD, PDHB and DLAT also significantly increased. These results indicate that copper deposition mediates TCA cycle disorders in psoriasis, activates cuproptosis processes, mediates oxidative stress and inflammatory infiltration, and ultimately promotes the pathological progression of psoriasis.

Although direct multi-omics evidence regarding the mechanism of cuproptosis in psoriasis was still lacking, integrated genomic, transcriptomic, and single-cell sequencing studies across various cancer fields including hepatocellular carcinoma, clear cell renal cell carcinoma, and breast cancer—suggested that the cuproptosis-related genes identified in this study (CD274, APOL6, LIAS, and PDHB) were highly sensitive to multiple clinical agents and exhibited significant potential for clinical intervention.[57–61] These genes were confirmed to be closely associated with responses to chemotherapeutic and targeted drugs such as docetaxel, doxorubicin, paclitaxel, and recovitin in the context of tumor microenvironment and cell death regulation. The correlation between low expression patterns of core cuproptosis genes such as DLAT and PDHB and drug sensitivity was validated across multiple independent cohorts. In the context of psoriasis, STAT1 and GBP1, as key effectors of the interferon signaling pathway, and CXCL10 and CD274 (PD-L1), as regulators of immune inflammation and checkpoint activity, were suggested to not only influence the fate of keratinocytes but also potentially modulate the local immunometabolic status, thereby rendering them sensitive

targets for potential pharmacological intervention. Thus, based on the crucial roles of these genes in drug response revealed by multi-omics analyses, targeting psoriasis-associated cuproptosis genes such as STAT1, CD274, LIAS, and PDHB was considered theoretically justified and is expected to open new avenues for combined immune-metabolic therapeutic strategies in psoriasis.

However, the dataset we adopted and the sample size of the animal experiments were not large, which might have restricted the reliability of the results. Furthermore, we have not further verified the results through clinical human experiments. Therefore, we will continue to explore in depth the mechanism of copper death in psoriasis in subsequent research.

Conclusion

In summary, we identified eight cuproptosis marker proteins in psoriasis through bioinformatics, including STAT1, DLD, GBP1, CXCL10, CD274, APOL6, LIAS, PDHB. Further analysis through machine learning identified three key PDCRGs, namely CD274, APOL6 and LIAS, which are mainly related to the TCA cycle pathway. In the psoriasis model mice induced by MIQ, the expression of these PDCRGs increased, promoting oxidative stress and inflammation levels, leading to the appearance of psoriasis characteristic skin lesions such as scales, infiltration, and erythema on the surface of the mouse skin. This has significant clinical value for targeted therapy of copper death-related genes for psoriasis.

Data Sharing Statement

All data generated or analyzed during this study are available from the corresponding author on reasonable request.

Ethics Approval and Consent to Participate

Animal experiment procedures were approved by the Animal Ethics Committee of Heilongjiang University of Chinese Medicine (SYXK-20250606). US National Institutes of Health Guide for the Care and Use of Laboratory Animals was followed in this study.

Author Contributions

Yingying Ma: Conceptualization and Writing – original draft

Jian Zhang: Data curation and Writing – original draft

Ying Sun: Data curation and Conceptualization, Supervision and Writing – review and editing

Jintong Yao: Formal analysis and Methodology and Writing – review and editing

Hailiang Wang: Validation and Writing – review and editing

Suqing Yang: Project administration and Writing – review and editing

All authors took part in drafting, revising or critically reviewing the article; gave final approval of the version to be published; have agreed on the journal to which the article has been submitted; and agree to be accountable for all aspects of the work.

Funding

This research was funded by the National Natural Science Foundation of China (81973846).

Disclosure

The author(s) report no conflicts of interest in this work.

References

1. Rendon A, Schäkel K. Psoriasis pathogenesis and treatment. *Int J Mol Sci*. 2019;20(6):1475. doi:10.3390/ijms20061475
2. Rousset L, Halioua B. Stress and psoriasis. *Int J Dermatol*. 2018;57(10):1165–1172. doi:10.1111/ijd.14032
3. Raharja A, Mahil SK, Barker JN. Psoriasis: a brief overview. *Clin Med Lond*. 2021;21(3):170–173. doi:10.7861/clinmed.2021-0257

4. Hawkes JE, Yan BY, Chan TC, et al. Discovery of the IL-23/IL-17 signaling pathway and the treatment of psoriasis. *J Immunol*. 2018;201(6):1605–1613. doi:10.4049/jimmunol.1800013
5. van der Fits L, Mourits S, Voerman JS, et al. Imiquimod-induced psoriasis-like skin inflammation in mice is mediated via the IL-23/IL-17 axis. *J Immunol*. 2009;182(9):5836–5845. doi:10.4049/jimmunol.0802999
6. Ten Bergen LL, Petrovic A, Krogh Aarebrot A, et al. The TNF/IL-23/IL-17 axis-head-to-head trials comparing different biologics in psoriasis treatment. *Scand J Immunol*. 2020;92(4):e12946. doi:10.1111/sji.12946
7. Boutet MA, Nerviani A, Gallo Afflitto G, et al. Role of the IL-23/IL-17 axis in psoriasis and psoriatic arthritis: the clinical importance of its divergence in skin and joints. *Int J Mol Sci*. 2018;19(2):530. doi:10.3390/ijms19020530
8. Wang Y, Zhang L, Zhou F. Cuproptosis: a new form of programmed cell death. *Cell Mol Immunol*. 2022;19(8):867–868. doi:10.1038/s41423-022-00866-1
9. Wang Y, Chen Y, Zhang J, et al. Cuproptosis: a novel therapeutic target for overcoming cancer drug resistance. *Drug Resist Updat*. 2024;72:101018. doi:10.1016/j.drup.2023.101018
10. Huang XY, Shen JY, Huang K, et al. Cuproptosis in cancers: function and implications from bench to bedside. *Biomed Pharmacother*. 2024;176:116874. doi:10.1016/j.biopha.2024.116874
11. Xu L, Cao X, Deng Y, et al. Cuproptosis-related genes and agents: implications in tumor drug resistance and future perspectives. *Front Pharmacol*. 2025;16:1559236. doi:10.3389/fphar.2025.1559236
12. Blackman RK, Cheung-Ong K, Gebbia M, et al. Mitochondrial electron transport is the cellular target of the oncology drug elesclomol. *PLoS One*. 2012;7(1):e29798. doi:10.1371/journal.pone.0029798
13. Yang L, Xie L, Li M, et al. Potential relationship between cuproptosis and sepsis-acquired weakness: an intermediate role for mitochondria. *Front Physiol*. 2025;16:1520669. doi:10.3389/fphys.2025.1520669
14. Tian Z, Jiang S, Zhou J, Zhang W. Copper homeostasis and cuproptosis in mitochondria. *Life Sci*. 2023;334:122223. doi:10.1016/j.lfs.2023.122223
15. Xue Q, Kang R, Klionsky DJ, et al. Copper metabolism in cell death and autophagy. *Autophagy*. 2023;19(8):2175–2195. doi:10.1080/15548627.2023.2200554
16. Masnikosa R, Cvetković Z, Pirić D. Tumor biology hides novel therapeutic approaches to diffuse large B-cell lymphoma: a narrative review. *Int J Mol Sci*. 2024;25(21):11384. doi:10.3390/ijms252111384
17. Fu S, Du H, Ling X, et al. Suppressing chondrocyte cuproptosis by syringaresinol-4-O-β-d-glucoside alleviates gouty arthritis. *Front Pharmacol*. 2025;16:1565422. doi:10.3389/fphar.2025.1565422
18. Lee JY, Hall JA, Kroehling L, et al. Serum amyloid A proteins induce pathogenic Th17 cells and promote inflammatory disease. *Cell*. 2020;180(1):79–91.e16. doi:10.1016/j.cell.2019.11.026
19. Qi RQ, Chen YF, Cheng J, et al. Elabela alleviates cuproptosis and vascular calcification in vitaminD3- overloaded mice via regulation of the PPAR-γ /FDX1 signaling. *Mol Med*. 2024;30(1):223. doi:10.1186/s10020-024-00997-3
20. Liu C, Fang Z, Yang K, et al. Identification and validation of cuproptosis-related molecular clusters in non-alcoholic fatty liver disease. *J Cell Mol Med*. 2024;28(3):e18091. doi:10.1111/jcmm.18091
21. Tsvetkov P, Coy S, Petrova B, et al. Copper induces cell death by targeting lipoylated TCA cycle proteins. *Science*. 2022;375(6586):1254–1261. doi:10.1126/science.abf0529
22. Qi W, Liu L, Zeng Q, et al. Contribution of cuproptosis and Cu metabolism-associated genes to chronic obstructive pulmonary disease. *J Cell Mol Med*. 2023;27(24):4034–4044. doi:10.1111/jcmm.17985
23. Yang M, Wang Y, He L, et al. Comprehensive bioinformatics analysis reveals the role of cuproptosis-related gene Ube2d3 in myocardial infarction. *Front Immunol*. 2024;15:1353111. doi:10.3389/fimmu.2024.1353111
24. Apaer A, Shi Y, Aobulitalifu A, et al. Identification of potential therapeutic targets for systemic lupus erythematosus based on GEO database analysis and Mendelian randomization analysis. *Front Genet*. 2024;15:1454486. doi:10.3389/fgene.2024.1454486
25. Feng S, Chen J, Qu C, et al. Identification of ferroptosis-related genes in schizophrenia based on bioinformatic analysis. *Genes*. 2022;13(11):2168. doi:10.3390/genes13112168
26. Tian Z, He W, Tang J, et al. Identification of important modules and biomarkers in breast cancer based on WGCNA. *Onco Targets Ther*. 2020;13:6805–6817. doi:10.2147/OTT.S258439
27. Theodore Armand TP, Nfor KA, Kim JI, et al. Applications of artificial intelligence, machine learning, and deep learning in nutrition: a systematic review. *Nutrients*. 2024;16(7):1073. doi:10.3390/nu16071073
28. Chen B, Khodadoust MS, Liu CL, et al. Profiling tumor infiltrating immune cells with CIBERSORT. *Methods Mol Biol*. 2018;1711:243–259.
29. Jia HY, Qiu HY, Zhang MD, et al. Lenalidomide attenuates IMQ-induced inflammation in a mouse model of psoriasis. *Biomed Pharmacother*. 2022;156:113883. doi:10.1016/j.biopha.2022.113883
30. Papp KA, Thoning H, Gerdes S, et al. Matching-adjusted indirect comparison of efficacy outcomes in trials of calcipotriol plus betamethasone dipropionate foam and cream formulations for the treatment of plaque psoriasis. *J DermatolTreat*. 2022;33(7):3005–3013. doi:10.1080/09546634.2022.2095330
31. Zhukov AS, Khairutdinov VR, Samtsov AV, et al. Preclinical efficacy investigation of human neutrophil elastase inhibitor sivelestat in animal model of psoriasis. *Skin Health Dis*. 2021;2(2):e90. doi:10.1002/ski2.90
32. Xu T, Zhong X, Luo N, et al. Review of excessive cytosolic DNA and its role in AIM2 and cGAS-STING mediated psoriasis development. *Clin Cosmet Invest Dermatol*. 2024;17:2345–2357. doi:10.2147/CCID.S476785
33. Pi W, Wu L, Lu J, et al. A metal ions-mediated natural small molecules carrier-free injectable hydrogel achieving laser-mediated photo-Fenton-like anticancer therapy by synergy apoptosis/cuproptosis/anti-inflammation. *Bioact Mater*. 2023;29:98–115. doi:10.1016/j.bioactmat.2023.06.018
34. Gao S, Ge H, Gao L, et al. Silk Fibroin Nanoparticles for Enhanced Cuproptosis and Immunotherapy in Pancreatic Cancer Treatment. *Adv Sci*. 2025;12(18):e2417676. doi:10.1002/advs.202417676
35. Huo S, Wang Q, Shi W, et al. ATF3/SPI1/SLC31A1 signaling promotes cuproptosis induced by advanced glycosylation end products in diabetic myocardial injury. *Int J Mol Sci*. 2023;24(2):1667. doi:10.3390/ijms24021667
36. Fang Z, Wang W, Liu Y, et al. Cuproptosis-related gene DLAT as a novel biomarker correlated with prognosis, chemoresistance, and immune infiltration in pancreatic adenocarcinoma: a preliminary study based on bioinformatics analysis. *Curr Oncol*. 2023;30(3):2997–3019. doi:10.3390/curroncol30030228

37. Tsvetkov P, Detappe A, Cai K, et al. Mitochondrial metabolism promotes adaptation to proteotoxic stress. *Nat Chem Biol*. 2019;15(7):681–689. doi:10.1038/s41589-019-0291-9
38. Solmonson A, DeBerardinis RJ. Lipoic acid metabolism and mitochondrial redox regulation. *J Biol Chem*. 2018;293(20):7522–7530. doi:10.1074/jbc.TM117.000259
39. Zhang X, Fan L, Wu J, et al. Macrophage p38α promotes nutritional steatohepatitis through M1 polarization. *J Hepatol*. 2019;71(1):163–174. doi:10.1016/j.jhep.2019.03.014
40. Liu H, Wang Y, Le Q, et al. The IFN-γ-CXCL9/CXCL10-CXCR3 axis in vitiligo: pathological mechanism and treatment. *Eur J Immunol*. 2024;54(4):e2250281. doi:10.1002/eji.202250281
41. Zhou B, Chen M, Hao Z, et al. Zinc-copper bimetallic nanoplatforms trigger photothermal-amplified cuproptosis and cGAS-STING activation for enhancing triple-negative breast cancer immunotherapy. *J Nanobiotechnol*. 2025;23(1):137. doi:10.1186/s12951-025-03186-4
42. Wang Y, Nguyen HP, Xue P, et al. ApoL6 associates with lipid droplets and disrupts Perilipin1-HSL interaction to inhibit lipolysis. *Nat Commun*. 2024;15(1):186. doi:10.1038/s41467-023-44559-3
43. Wang H, Yang Z, He X, et al. Cuproptosis related gene PDHB is identified as a biomarker inversely associated with the progression of clear cell renal cell carcinoma. *BMC Cancer*. 2023;23(1):804. doi:10.1186/s12885-023-11324-0
44. García-Fuentes E, Santiago-Fernández C, Gutiérrez-Repiso C, et al. Hypoxia is associated with a lower expression of genes involved in lipogenesis in visceral adipose tissue. *J Transl Med*. 2015;13:373. doi:10.1186/s12967-015-0732-5
45. Yongzhong C, Hui C, Luting Z, et al. Mechanism of jianxin granules in the treatment of heart failure based on proteomics and metabolomics. *Chin Med*. 2024;19(1):165. doi:10.1186/s13020-024-01009-6
46. Xing T, Li L, Chen Y, et al. Targeting the TCA cycle through cuproptosis confers synthetic lethality on ARID1A-deficient hepatocellular carcinoma. *Cell Rep Med*. 2023;4(11):101264. doi:10.1016/j.xcrm.2023.101264
47. Cobine PA, Brady DC. Cuproptosis: cellular and molecular mechanisms underlying copper-induced cell death. *Mol Cell*. 2022;82(10):1786–1787. doi:10.1016/j.molcel.2022.05.001
48. Li SR, Bu LL, Cai L. Cuproptosis: lipoylated TCA cycle proteins-mediated novel cell death pathway. *Signal Transduct Target Ther*. 2022;7(1):158. doi:10.1038/s41392-022-01014-x
49. Li L, Zhou H, Zhang C. Cuproptosis in cancer: biological implications and therapeutic opportunities. *Cell Mol Biol Lett*. 2024;29(1):91. doi:10.1186/s11658-024-00608-3
50. Dreishpoon MB, Bick NR, Petrova B, et al. FDX1 regulates cellular protein lipoylation through direct binding to LIAS. *bioRxiv [Preprint]*. 2023.
51. Liu X, Si W, He L, et al. The existence of a nonclassical TCA cycle in the nucleus that wires the metabolic-epigenetic circuitry. *Signal Transduct Target Ther*. 2021;6(1):375. doi:10.1038/s41392-021-00774-2
52. Sharma S, Bhattarai S, Ara H, et al. SOD2 deficiency in cardiomyocytes defines defective mitochondrial bioenergetics as a cause of lethal dilated cardiomyopathy. *Redox Biol*. 2020;37:101740. doi:10.1016/j.redox.2020.101740
53. Hu Q, Zhang X, Huang J, et al. The STAT1-SLC31A1 axis: potential regulation of cuproptosis in diabetic retinopathy. *Gene*. 2024;930:148861. doi:10.1016/j.gene.2024.148861
54. Qi H, Zhu D. Oncogenic role of copper-induced cell death-associated protein DLD in human cancer: a pan-cancer analysis and experimental verification. *Oncol Lett*. 2023;25(5):214. doi:10.3892/ol.2023.13800
55. Ding RL, Zheng Y, Bu J. Exploration of the biomarkers of comorbidity of psoriasis with inflammatory bowel disease and their association with immune infiltration. *Skin Res Technol*. 2023;29(12):e13536. doi:10.1111/srt.13536
56. Yao J, Gan W, Sun J, et al. APOL6 as a potential biomarker of immuno-correlation and therapeutic prediction in cancer immunotherapy. *Medicine*. 2025;104(19):e42406. doi:10.1097/MD.0000000000042406
57. Fu J, Wang S, Li Z, et al. Comprehensive multiomics analysis of cuproptosis-related gene characteristics in hepatocellular carcinoma. *Front Genet*. 2022;13:942387. doi:10.3389/fgene.2022.942387
58. Chen L, Hu Y, Li Y, et al. Integrated multiomics analysis identified comprehensive crosstalk between diverse programmed cell death patterns and novel molecular subtypes in Hepatocellular Carcinoma. *Sci Rep*. 2024;14(1):27529. doi:10.1038/s41598-024-78911-4
59. Wu J, Wang S, Liu Y, et al. Integrated single-cell and bulk characterization of cuproptosis key regulator PDHB and association with tumor microenvironment infiltration in clear cell renal cell carcinoma. *Front Immunol*. 2023;14:1132661. doi:10.3389/fimmu.2023.1132661
60. Zhu M, Li Y, Wang Y, et al. Multi-omics analysis uncovers clinical, immunological, and pharmacogenomic implications of cuproptosis in clear cell renal cell carcinoma. *Eur J Med Res*. 2023;28(1):248. doi:10.1186/s40001-023-01221-4
61. Fang D, Zhou Y, Liao F, et al. Identification and characterization of cuproptosis related gene subtypes through multi-omics bioinformatics analysis in breast cancer. *Discov Oncol*. 2025;16(1):171. doi:10.1007/s12672-025-01952-2